

©[2010]

Chao-ting Wang

ALL RIGHTS RESERVED

RICIN-A-CHAIN (RTA) INHIBITS UNFOLDED PROTEIN RESPONSE (UPR) IN
MAMMALIAN CELLS

by

CHAO-TING WANG

A thesis submitted to the

Graduate School-New Brunswick

Rutgers, The State University of New Jersey

in partial fulfillment of the requirements

for the degree of

Master of Science

Graduate Program in Nutritional Sciences

written under the direction of

Dr. Wendie S. Cohick

and approved by

New Brunswick, New Jersey

[October, 2010]

ABSTRACT OF THE THESIS

Ricin-A-chain (RTA) inhibits the unfolded protein response (UPR) in mammalian cells.

BY CHAO-TING WANG

Thesis Director:

Dr. Wendie S. Cohick

Ricin, a type II ribosome-inactivating protein, has been used as a biochemical weapon due to its ability to inhibit protein synthesis and induce cytotoxicity. The unfolded protein response (UPR) is a survival response that helps cells to recover from stress that occurs following the accumulation of misfolded proteins in the ER. Failure to recover from ER stress can lead to apoptosis. In yeast, ricin-A-chain (RTA), the enzymatic component of ricin, inhibits the unfolded protein response (UPR). However, the ability of RTA to affect UPR has not been investigated in mammalian cells. The goals of this project were to determine if RTA could inhibit the UPR in mammalian cells and if altering the UPR affected RTA cytotoxicity. The UPR consists of three signaling cascades, IRE1, PERK, and ATF6. In HeLa cells, a human cervical carcinoma cell line, we found that RTA could inhibit tunicamycin (Tm)-induced IRE1 phosphorylation and XBP-1 mRNA splicing at 4 h. A similar effect was observed in the non-transformed mammary epithelial cell line MAC-T. RTA also inhibited the ability of dithiothreitol (DTT) to activate the PERK pathway in HeLa cells, as shown by inhibition of DTT-induced eIF2 α phosphorylation at 4 h. In both cell types, RTA decreased expression of

the downstream chaperone BiP in response to Tm. To determine if inhibition of the IRE1 and PERK pathways by RTA affected its cytotoxicity, cells were treated with RTA in combination with DTT or Tm. Cleavage of both caspase-3 and -7 was greater in both HeLa and MAC-T cells when they were treated with RTA and DTT or RTA and Tm compared to cells treated with RTA, DTT, or Tm alone. These results indicate that RTA is more cytotoxic when UPR is inhibited.

Table of Contents

Abstract.....	ii
Table of Contents	iv
List of Figures.....	vii
Chapter 1	1
Ricin.....	2
Structure and Function.....	2
Trafficking - Retrograde transport	2
Ribosome Inactivation	4
Immunotoxin/ Cancer therapy	5
ER stress.....	6
ER functions.....	6
ER stress/Unfolded protein response (UPR).....	6
ER stress-induced apoptosis	8
ER stress-related diseases	9
ER stress response transducer - IRE1	10
Yeast IRE1	10
Mammalian IRE1	11
IRE1 structure and activation.....	11
Splicing.....	13
pXBP1(s) up-regulates ER-stress related genes	13
Unspliced Hac1 and XBP1	14
JNK activation	15

ER stress response transducer – ATF6	15
ATF6 activation.....	15
ATF6 cleavage and translocation	16
p50ATF6-induced genes	17
Regulation of ATF6.....	17
ER stress transducer - PERK	18
Protein synthesis inhibition/ATF4 expression	18
Nrf2.....	19
Regulation of the PERK pathway.....	20
Objectives of the thesis	20
Chapter 2.....	21
Introduction.....	22
Materials and Methods.....	23
Reagents.....	23
Cell Culture.....	24
Western Blotting	24
RT-PCR assay to detect XBP1 splicing	25
Quantitative(q) RT-PCR.....	25
Statistical analysis.....	26
Results.....	27
RTA inhibits XBP1 splicing in mammalian cells.....	27
RTA inhibits Tm-induced phosphorylation of IRE1	28
RTA inhibits the DTT-induced phosphorylation of eIF2 α	29
RTA inhibits Tm-induced BiP mRNA expression.....	29

Inhibition of ER stress sensitizes cells to RTA-induced cytotoxicity	30
Discussion.....	30
Figures.....	35
Abbreviation List	48
References.....	50

List of Figures

Figure 1. Signaling pathways of UPR.....	35
Figure 2. Downstream signaling of UPR pathway.....	36
Figure 3. Primer design for XBP1 splicing assay using RT-PCR.....	37
Figure 4. Primer design for XBP1 qRT-PCR	38
Figure 5 Exogenous RTA inhibits tunicamycin (Tm)-induced XBP1 splicing in MAC-T cells	39
Figure 6. Exogenous RTA inhibits Tm-induced XBP1 splicing in HeLa cells	40
Figure 7. Effect of exogenous RTA on thapsigargin (Tg) and DTT-induced XBP1 splicing in HeLa cells	41
Figure 8. Exogenous RTA inhibits Tm-induced phosphorylation of IRE1 in HeLa cells.	42
Figure 9. Exogenous RTA inhibits DTT-induced phosphorylation of eIF2 α in HeLa cells	43
Figure 10. Exogenous RTA inhibits Tm-induced BiP mRNA expression in MAC-T and HeLa cells	44
Figure 11. Exogenous RTA does not inhibit Tg-induced BiP mRNA expression in HeLa cells	45
Figure 12. DTT does not induce BiP mRNA in HeLa cells at 30 mins.	46
Figure 13. Caspase cleavage is enhanced in cells treated with both exogenous RTA and UPR-inducing agents	47

Chapter 1

Review of Literature

Ricin

Ricin is a 64 kDa glycosylated protein that is a byproduct of oil extraction from the castor bean (*Ricinus communis*) which originates from Asia and Africa. It can be destroyed during the heating process of the oil extraction. It may cause poisoning through inhalation, injection, or ingestion. Its symptoms include difficulty breathing, severe dehydration, hypotension, and the malfunction of multiple organs, such as lung, liver, spleen, and kidney (1-4). Due to its toxicity, some terrorist or military organizations have used it as a weapon during warfare.

Structure and Function

Ricin, a type II ribosome-inactivating protein (RIP), is composed of two polypeptide chains linked by disulfide bonds (5). Such structure is similar to abrin, a natural toxin from the seed of rosary peas, and diphtheria toxin, a bacterial toxin from *Corynebacterium diphtheriae*. Ricin-A-chain (RTA) is the enzymatic part of ricin which can inactivate the 60S ribosomal unit and cause inhibition of protein synthesis. The N-glycosidase activity of RTA depurinates the adenine (A4324) on the exposed loop, the sarcin-ricin loop, of the 28S rRNA (6). Ricin-B-chain (RTB) contains galactose binding sites which can bind to the galactose-containing glycoproteins and glycolipids on the cell surface to help the holotoxin enter the cells.

Trafficking - Retrograde transport

The first discovery of retrograde transport was reported in a study on Shiga toxin (7), a bacterial toxin produced by certain species of *E. coli*. Shiga toxin enters the cell through endocytosis after binding to the cell membrane. Inside the cell, it undergoes retrograde

transport through the Golgi apparatus into the ER and then into the cytosol. This pathway also accounts for the cytotoxicity of ricin (8). After the galactose-binding site on RTB binds to the cell membrane, the holotoxin is internalized mainly through clathrin-dependent endocytosis to be taken up into endosomes (9). However, ricin was also internalized in studies where clathrin-dependent endocytosis was blocked by acidification of the cytosol (inhibits the formation of clathrin-coated pits) (10), potassium depletion (removes clathrin-coated pits from the membrane) (11-12), or overexpression of mutant dynamin (important in clathrin-mediated endocytosis) (13), indicating that ricin can be internalized by clathrin-independent pathways. Once internalized, ricin is routed by the endosomal system. The majority of the protein is either recycled and transported back to the cell surface or degraded by lysosomes, with only a small amount of ricin (5%) delivered to the trans-Golgi network (14).

The mechanism by which ricin is transported to the trans-Golgi network is not completely defined. Rab9 is located on the surface of late endosomes and helps transport mannose 6-phosphate receptors from late endosomes to Golgi (15). Rab9 has been considered as one of the candidates of ricin transport. However, mutant Rab9S21N could not block ricin transport to Golgi (16). A recent study has shown that two small molecules can inhibit ricin intoxication by blocking this endosome-Golgi retrograde route (17), but the mechanism is still unresolved. Once ricin enters the Golgi it must be transported to the endoplasmic reticulum (ER). It has been reported that the KDEL (Lys-Asp-Glu-Leu) receptor may be important for this retrograde transport (18-19). However, unlike cholera toxin, a bacterial toxin secreted by *Vibrio cholerae*, ricin does not contain the KDEL sequence which is a signal for protein retention in the ER. One possibility is that ricin

binds to the intracellular proteins that contain the KDEL sequence in the Golgi and is then transported to the ER. One likely candidate is calreticulin, which shuttles between the Golgi and the ER and also contains free galactose residues that can bind RTB (18, 20). It has been shown that ricin could interact with calreticulin, which is abundant in vivo (21) although another study showed that cells lacking calreticulin were still sensitive to ricin (22).

It has been reported that reduction of the disulfide bond between the RTA and RTB chains is necessary for ricin cytotoxicity (23-24). After entering the ER, the protein disulfide isomerase (PDI) reductively cleaves the disulfide bond between the holotoxin and releases RTA. The free RTA interacts with the negatively-charged ER membrane lipids which induces a conformational change and causes RTA to be partially unfolded (25). This misfolding process may allow RTA to be exported to the cytosol by the protein quality control of the ER, or ERAD (ER-associated degradation), which sends misfolded proteins for degradation. However, RTA can successfully escape from proteolytic degradation because of its low content of lysine (only two) (26). This partially unfolded RTA can rapidly refold in the cytosol with the facilitation of ribosomes (27). The refolded RTA in the cytosol has more resistance to proteolytic degradation than the unfolded RTA (28) and retains full enzymatic activity.

Ribosome Inactivation

In the cytosol, RTA targets the 28S rRNA of the 60S ribosomal subunit. The N-glycosidase activity of RTA depurinates the adenine (A4324 in rat 28S RNA) on the exposed loop, the sarcin-ricin loop, of the 28S rRNA (6). The targeted sequence of the sarcin-ricin loop (AGUACGAGAGGAAC) is highly conserved between eukaryotes and

prokaryotes and is essential for the binding of translation elongation factors (29). The RTA-modified rRNA has low affinity for elongation factor binding and consequently causes protein biosynthesis inhibition (30). The enzymatic activity of RTA is so efficient that one RTA molecule can depurinate 2000 ribosomes per minute which contributes to its high cytotoxicity (31). However, recent work in yeast suggests that protein synthesis inhibition may not be sufficient for cytotoxicity (32). While RTA can induce apoptosis in mammalian cells (33), the link between ribosome depurination and cell death is presently unknown.

Immunotoxin/ Cancer therapy

It has been shown that tumor cells respond faster to protein synthesis inhibition by ricin compared with normal cells (34). Thus, ricin has been proposed as a potential treatment for cancer. Many studies have explored the idea of conjugating ricin with antibodies or growth factors (23, 35-36). However, there are some issues that interfere with development of this approach as a cancer therapy. It has been shown that the holotoxin can bind to cells nonspecifically, and even without the RTB binding domain, RTA could be taken up by some cells through its glycosylated residues. This led researchers to chemically deglycosylate RTA or holotoxin to block carbohydrate binding, which successfully prolonged the half-life of the immunotoxin in the blood of mice without reducing its ability to kill the tumor cells (37-39). In addition to the issue of binding specificity, immunogenicity, and vascular leak syndrome (VLS) (40-41), are problems that must be overcome before ricin will be useful as an immunotoxin.

ER stress

ER functions

The endoplasmic reticulum (ER) is a membrane-surrounded organelle which functions in calcium homeostasis, secretory and membrane protein synthesis, post-translational protein modification, and biosynthesis of lipid and sterols. In mammalian cells, the ER functions as the main storage site of intracellular Ca^{2+} , which enters the ER through SERCA (ER-localized transmembrane P-type ATPase). This intracellular Ca^{2+} is a crucial component of intracellular signal transduction pathways (42). Ca^{2+} also binds to ER-resident proteins, such as BiP and calnexin, to facilitate protein folding in the ER in a Ca^{2+} -dependent manner (43-45). Newly synthesized proteins destined for the ER cross the ER membrane via the Sec61 complex. Once inside the ER lumen, protein folding is facilitated by foldases and chaperones and modifications, such as N-linked glycosylation and the formation of disulfide bonds are instituted. The ER has the ability to monitor if the protein is completely and appropriately folded. If it is, the protein is transported to the Golgi; if not, it is retained in the ER by reglycosylation by UGGT (UDP-glucose: glycoprotein glucosyltransferase). The reglycosylated proteins can rebind chaperones (46) or alternatively, be degraded by ERAD (47-48).

ER stress/Unfolded protein response (UPR)

Any perturbations of the functions described above can disrupt ER homeostasis and cause ER stress. The first description of ER stress involved the viral transformation of eukaryotic cells. This led to an increase in glucose metabolism and caused glucose deprivation, further inducing expression of the glucose-regulated protein family (GRPs)

which are stress-induced proteins located in the ER (49-50). Moreover, the mechanism of protein folding in the ER requires energy, therefore glucose deprivation causes a decrease in energy supply and slows the process of folding, causing proteins to accumulate in the ER (51). Calcium depletion is another major reason for ER stress. As mentioned above, Ca^{2+} binds to the ER-resident proteins that are important in protein folding. In addition, Ca^{2+} depletion inhibits the binding of UGGT to incompletely-folded proteins by inactivating UGGT and repressing the import of UDP glucose. This results in inhibition of the refolding and degradation process, causing large amounts of unfolded proteins to be retained in the ER (52). Therefore, accumulation of unfolded protein in the ER lumen is a crucial component of ER stress.

Once ER stress occurs, cells have several mechanisms to regain homeostasis. These responses are collectively called the ER stress response or UPR, although cells respond differently to various causes of ER stress. The transcription of ER-localized chaperones and folding enzymes increases to accelerate the efficiency of protein folding (53-54), but general protein translation is shutoff to relieve the accumulation of protein in the ER lumen (55). Synthesis of phospholipids increases to expand the capacity of the ER. Moreover, the misfolded proteins are retrotranslocated to the cytoplasm to be degraded by the proteasome by ERAD (47-48). These responses are elicited to restore ER homeostasis. However, if cells cannot recover from ER stress through these responses, they eventually undergo apoptosis to remove the unhealthy cells.

In mammalian cells UPR requires three main signal transducers to be executed: IRE1 (inositol-requiring protein 1), ATF6 (activating transcription factor 6), and PERK (PKR-like ER kinase) (see Figures 1 and 2). This contrasts with yeast, which has only the

IRE1 pathway to respond to ER stress (56). It has been reported (57) that these three stress-response transducers are activated in a time-frame such that PERK may be the first to sense the stress and be activated to attenuate general translation via inactivation of eukaryotic elongation factor 2 α (eIF2 α) to alleviate the load on ER chaperones. If the stress persists, ATF6 is activated to induce chaperone production, e.g. BiP, Grp94, and calreticulin, which facilitate protein folding in the ER lumen. IRE1 may be the last protection from ER stress, and functions to induce additional chaperones and ERAD components, such as EDEM (ER degradation-enhancer mannosidase-like alpha 1) (57) and, an HMG-CoA reductase degradation1 (HRD1) protein (58-59), which accelerate the clearance of misfolded proteins from the ER. However, this order of time-dependent activation may vary between different cell types, species or different causes of ER stress. For example, another study (60) provided different temporal profiles of activation and subsequent turnover for these three transducers. They showed that while all three pathways are activated at the early stage of ER stress, IRE1 is attenuated within 8 h while ATF6 and PERK persist longer, with the PERK pathway activated through 30 h.

ER stress-induced apoptosis

Under ER stress, both pro-apoptotic and anti-apoptotic pathways are activated (61-62). IRE1 can induce JNK activation by binding with TRAF2 (TNF receptor-associated factor 2) (63-64) and activate caspase-12 by cleaving procaspase-12. JNK activation may phosphorylate the pro-apoptotic proteins, BIM and BMF, to induce BAX-induced apoptosis (65-66). Moreover, it has been reported that ER stress also induces other pro-apoptotic BH3-only proteins, such as BIM, PUMA, and NOXA through p53 (67-69). The PERK and ATF6 pathways induce CHOP/GADD153 which represses the transcription

of the anti-apoptotic protein, Bcl-2 and further activates BAX/BAK, thus inducing apoptosis (70-71). Since the ER is the major intracellular storage site of Ca^{2+} , ER stress-induced loss of Ca^{2+} from the ER lumen also triggers apoptosis. The cytosolic calcium-dependent protease calpain senses the depletion of Ca^{2+} in the ER and activates caspase-12, which leads to activation of caspase-9 and -3 (72). In addition, the cytosolic Ca^{2+} is then taken up by the mitochondria, causing collapse of the inner membrane potential to induce cell death as well (73). Therefore, the balance of Bcl-2 and BH3-only proteins is crucial for whether the cells undergo apoptosis or recover from the stress.

ER stress-related diseases

UPR is relevant to many diseases, such as cancer, type I and II diabetes, polyglutamine disease, etc. whether it is the cause or the consequence of these diseases. Pancreatic β islet cells have well-developed ER due to the large amount of secretory insulin produced there. PERK-null mice, due to apoptosis of their pancreatic β islet cells, present with type I diabetes (74-75). Several human families have been identified with this disorder, called Wolcott-Rallison syndrome, which is due to the inherent loss-of-function of the PERK gene (76). ER stress is also induced by a high-fat diet and further develops into type II diabetes in mice. PERK is activated and Grp78 (also known as BiP) is up-regulated in obese mice on the high-fat diet (77). In addition, ER stress-induced JNK activation can cause insulin resistance (78). Cancer is another disease which is highly relevant to ER stress. It has been shown that Grp78 and XBP1 are highly expressed in the presumptive ischaemic areas of tumors and hypoxic cancer cells *in vivo* and *in vitro* (79-80). Other studies have also shown that tumorigenic activity is significantly reduced in mice with a deficiency of GRP78, XBP-1, or PERK (81-83).

ER stress response transducer - IRE1

Yeast IRE1

Ire1p/Ern1p, ER-associated type I transmembrane protein kinase, was the earliest discovered ER stress-induced pathway in the yeast *Saccharomyces cerevisiae* (84-85). It is the homologue of the regulated endoribonuclease, RNaseL which acquired a protein kinase domain and ribonuclease activity. During ER stress, the luminal domain of IRE1 senses the disturbed environment in the ER, becomes oligomerized and then autophosphorylates its own kinase domain at two sites, Ser840 and Ser841, to activate the sequence-specific endoribonucleolytic activity (86-87). RNaseL lacks these catalytic kinase and autophosphorylation activities (88). This endoribonuclease located on the C-terminal non-luminal side of IRE1 (89) excises a small intron of the pre-existing mRNA *Hac1*. The two remaining exons (90-92) are joined by tRNA ligase which is encoded by RLG1 (93) and translated to produce a transcription factor that binds to the 22 bp UPR element of the promoter region of the *KAR2* gene, the yeast homologue of Grp78/BiP and two other PDI-like genes in yeast (90, 94).

Hac1p is a basic-region leucine-zipper (bZIP) transcription factor in yeast which is only present during ER stress (90). During ER stress, the intron of *HAC1* mRNA is spliced at the 3' end (252 nucleotides) by IRE1 causing the size to be reduced from 1.4-kb to 1.2-kb (90). Moreover, this splicing mechanism is independent of the spliceosome (93). After splicing, Hac1p, a 238 amino acid protein, is produced to up-regulate other ER-stress related genes in yeast. However, in the resting state, the *Hac1* mRNA with the 252-nt intron stalls on the ribosomes and is not translated into protein (95).

Mammalian IRE1

In humans and mice, there are two identical isoforms of IRE1, IRE1 α and IRE1 β , which are highly conserved with yeast. These two isoforms are encoded from two different genes. IRE1 α is generally found throughout the body while IRE1 β is only found in the epithelial cells of the gut (96-97). It has been shown that, just like yeast IRE1, the RNase domain of mammalian IRE1 also can be activated by autophosphorylation of its kinase domain (96) due to the most conserved domains from the yeast: RNaseL-like domain and the kinase domain in the C-terminus of the protein. It has been shown that overexpressing either of these two isoforms can induce BiP expression by activating its promoter region (96-97). IRE1 β has also been reported to trigger CHOP/GADD153 gene activation (97-98).

XBPI is the homologue of *Hac1* in mammalian cells and is also a substrate for the ribonuclease function of IRE1. During ER stress, a 26-nt intron of *XBPI* mRNA is spliced to yield a 376 amino acid protein. This is larger than the unspliced form of the XBPI protein, which is 261 amino acids, due to a reading frame shift after splicing (99-101). This spliced XBPI protein can also function as a transcription factor to regulate other ER stress-induced genes, such as Grp78/BiP (99).

IRE1 structure and activation

There are luminal N-terminal and cytosolic domains in IRE1. ER stress induces the dimerization of the luminal domain and further activates the cytosolic domain to cleave the mRNA substrate. This N-terminal luminal domain (NLD) is composed of 367 amino acid residues with three main β -sheet motifs that are linked by α -helix arrangements. This structure is conserved between human and yeast IRE1, though there are some differences

observed (102-103). Some groups proposed that the dimerization of the NLD of yeast IRE1 is induced by its binding with unfolded proteins present in the ER (102, 104). However, another group found that the purified NLD of IRE1 can get dimerized without the presence of other proteins in vitro and the structure of the human NLD is too narrow for peptide binding. Moreover, replacement of the yeast NLD with the human sequence can still induce the UPR pathway, suggesting that the binding of peptide is not necessary for IRE1 activation, at least in mammalian cells (103, 105). In contrast, it has been determined that BiP association is a negative regulator of the ER stress pathway (106-107). It has also been shown that the binding site of BiP in human IRE1 is spatially conserved in yeast (102). IRE1 mutants with reduced ability to interact with BiP can still be activated in the absence of unfolded protein (105). Therefore, these researchers suggested that the unfolded protein induced-BiP dissociation from the monomeric IRE1 is required for the dimerization of IRE1.

The cytosolic domain of IRE1 contains the bilobal N-terminal kinase domain and, in its C-terminal lobe, is followed by a conserved 132 residue globular kinase-extension nuclease (KEN) domain. After the dimerization of the luminal domain, the juxtaposition of two cytosolic kinase domains promote the trans-autophosphorylation of an activation segment between the N- and C- lobe of the kinase domain. Following this event, ADP/ATP binds to the nucleotide binding cleft which facilitates dimerization of the cytosolic domain of IRE1 and this IRE1 dimer or oligomer activates the function of ribonuclease on the KEN domain (108). Mutation of this dimer interface residue would destroy the endonuclease activity of IRE1 (108).

Splicing

Xbp1 mRNA in mammalian cells reveals a stem-loop structure in both the 5' and 3' splice sites which is very similar to yeast *Hac1*. After binding to the KEN domain of the activated IRE1 dimer or oligomer, Ire1 cleaves the third nucleotide, G, of the 7-nucleotide loop with consensus sequence CNGNNGN where N can be any nucleotide of the mammalian *XBP1* and yeast *Hac1* mRNA. This intron fragment between the two cleavage sites is removed from the target gene (109). The remaining two exons are joined together by tRNA ligase Rlg1 in yeast (93), however, the metazoan homolog of Rlg1 has not been identified (108). After splicing, the reading frame in the C-terminus is changed. This type of splicing is called frame switching splicing (57) or cytoplasmic splicing (110). As mentioned above, unlike yeast *Hac1*, the unspliced *xbp1* is also translated into protein, but is rapidly degraded by the proteasome and cannot be observed by western blot (99, 101).

pXBPI(s) up-regulates ER-stress related genes

After being translated, the protein of spliced *XBPI*, *pXBPI(s)*, translocates into the nucleus and functions as a transcription factor to up-regulate UPR related genes by binding to the *cis*-acting element ERSE, the ER stress response element (CCAAT-N₉-CCACG) (99, 111-112), located on the promoter region of BiP and many other ER stress genes, such as Grp94, p58IPK, and *XBPI* itself (99, 113). It has been reported that the binding of *pXBPI(s)* to the CCACG sequence of the ERSE requires the binding of another transcription factor, NF-Y (also known as CBF) to the CCAAT region of this consensus sequence (99, 112, 114). *pXBPI(s)* can also bind to two other elements, ERSEII, which contains the ATTGG-N-CCACG consensus sequence, and UPRE, which contains the

TGACGTGG/A consensus sequence, to up-regulate other ER stress related genes, such as Herp, EDEM, and HRD1. NF-Y is not essential for pXBP1 activation of genes containing these two sequences (99, 114). It has been shown that in IRE1 α -null murine embryonic fibroblasts (MEF) cells, the tunicamycin-induced expression of a 5x ATF6 reporter gene was totally abolished. This suggests that during ER stress, the IRE1/XBP1 pathway may regulate another UPR pathway, the ATF6 pathway (100, 115).

Unspliced Hac1 and XBP1

Unspliced *Hac1* contains the 5' 252 nt untranslated region that is spliced out by Ire1, so it is not translated into protein (110). Unlike yeast, the mammalian unspliced *XBP1* can be translated into protein, pXBP1(U), because the 26-nt splicing sequence is too small to form the translation inhibitory structure (99). Both the pXBP1(S) and pXBP1(U) share the N-terminal 166 aa containing the bZIP domain, but the pXBP1(U) has two unique domains that are different from pXBP(S): the nuclear export signal (NES) and the degradation domain while the pXBP1(S) only has the nuclear localization signal. These two exclusive domains allow the pXBP1(U) to shuttle between the nucleus and cytoplasm and to be degraded by the proteasome (116). In the later stages of ER stress, pXBP1(S) gradually decreases while the pXBP1(U) increases, suggesting that IRE1 is inactivated while *XBP1* mRNA is still transcribed (116). pXBP1(U) then formed a complex with pXBP1(S) to transport pXBP1(S) out of the nucleus via its NES, targeting it for degradation by the proteasome via its degradation domain. This negative feedback loop shuts off the IRE1/XBP1 pathway of the UPR. This is important for cell homeostasis as the over-expressed chaperones in the unstressed situation are toxic to cells and repress cell growth (56).

JNK activation

IRE1 can also induce apoptosis via the JNK signaling pathway if ER stress is prolonged. After IRE1 gets activated, IRE1 forms a heterotrimeric complex by associating with TRAF2 and ASK1 (apoptosis signal-regulating kinase 1) to activate JNK and caspase-7 and -12 and initiate programmed cell death (63-64, 117). However, several groups have shown that this process is involved with AIP (ASK interacting protein1) (118); the mechanism by which this complex induces JNK activation is still unclear.

ER stress response transducer – ATF6

Previous studies (112, 115, 119-120) determined that ATF6 is a target of UPR since the active form of ATF6 could induce the expression of Grp78, Grp94 and calnexin genes. ATF6 is a 670-amino acid type II transmembrane glycoprotein with a single transmembrane domain in the ER. Its C-terminus (270 amino acids) in the ER lumen senses ER stress while its cytosolic N-terminal domain (amino acids 1-373) is a transcription factor belonging to the basic-leucine zipper (bZIP) family. The 21 amino acids between the two represent the transmembrane area (119). There are two isoforms of ATF6: α and β . Each is ubiquitously expressed and contains the bZIP domain and a DNA binding domain in the internal region. However, an 8 amino acid sequence located in the transcription-activating domain of ATF6 α is absent in ATF6 β (121). This sequence causes ATF6 α to exhibit much stronger transcriptional activation than ATF6 β .

ATF6 activation

N-linked glycosylation of the 670-amino acid ATF6 protein results in a size of 90 kDa when determined by denaturing SDS-PAGE. This specific glycosylation sequence is

composed of Asparagine-N-Serine/Threonine where N can be any amino acid other than Proline (122). In human ATF6, these three amino acids are respectively located at positions 472, 584, and 643 in the ER luminal domain, and are conserved in mouse ATF6. This glycosylation is important for sensing stress in the ER lumen and also for ATF6 activation. Under ER stress, compared to the fully glycosylated ATF6, the newly synthesized ATF6 is underglycosylated which is easier to translocate to Golgi to be processed (123).

Another mechanism that regulates ATF6 activation is Grp78/BiP which under normal conditions binds to the luminal domain of ATF6 to inhibit the Golgi localization signal (GLS) 1 and 2. During ER stress, BiP dissociates from ATF6 and binds to misfolded proteins. This dissociation allows ATF6 to translocate to the Golgi and be processed (124-125). It has been shown that overexpressed BiP can delay ATF6 activation (125).

ATF6 cleavage and translocation

After BiP dissociates from ATF6 during ER stress, free ATF6 is subsequently transported to the cis-Golgi compartment through COP II cytosolic protein complex at the ER exit site (125-126). Residues 468-500 are required for this translocation since an ATF6 mutant that lacks this region is still retained in the ER (124). In the Golgi, ATF6 is cleaved at sequence RRHLL (amino acids 415-419) within the luminal domain by site-1 protease (S1P) and also cleaved within the transmembrane domain (amino acids 391-394) by site-2 protease (S2P) (112, 115, 119-120). These two proteases also cleave sterol-response-element binding protein (SREBP) which regulates cholesterol biosynthesis (127-128). This C-terminus deletion of ATF6 yields a 50-kDa soluble cytoplasmic protein (p50ATF6) which contains several nuclear localization signals (NLS) and a bZIP

domain between amino acids 308-369. The N-terminus then translocates to the nucleus via its interaction with importin, the NLS receptor, and the basic residue cluster on ATF6 (129).

p50ATF6-induced genes

In the nucleus, ATF6 acts as a transcription factor to induce genes by binding to the sequence CCACG on the ERSE. As in the case of the spliced form of XBP1, this process requires the binding of NF-Y on the CCAAT of the ERSE (112). There are 9 nucleotides between these two binding regions that are important for ERSE activity. Unlike XBP1, ATF6 cannot recognize the UPRE. Using microarray, Yamamoto's group (58) found 30 genes out of 14,729 genes that are ATF6 target genes, including seven for ER chaperones such as BiP, and six for ER proteins such as CHOP. ATF6 also can induce five ERAD components by forming a heterodimer with XBP1 (130). It has also shown that *XBPI* is a target of ATF6. *XBPI* mRNA expression is induced by ATF6 and then spliced by IRE1 (51, 99). During ER stress, this pathway precedes activation of the IRE1/XBP1 pathway since ATF6 does not need to be newly synthesized. Therefore, in the early stages of ER stress, ATF6 induces the production of chaperones to assist protein folding. However, if the stress cannot be relieved, XBP1(S) is translated, which results in the synthesis of more chaperones such as BiP. At the same time, XBP1 can induce EDEM, to get rid of misfolded proteins through ERAD (57).

Regulation of ATF6

Thuerauf's group (131) proposed that ATF6 β needs more time to be cleaved and yield the N-terminus relative to ATF6 α . Since ATF6 β has a relatively lower degree of

transcriptional activation, ATF6 β could be a dominant-negative modulator of ATF6 α in the later stages of ER stress.

ER stress transducer - PERK

A second mammalian-specific ER-response protein is PERK which is an ER resident type I transmembrane kinase (132). The luminal domain of PERK shows limited homology to the IRE1 luminal domain, indicating that they share similar mechanisms in response to ER stress. Both PERK and IRE1 need BiP to be dissociated from their luminal domains to allow oligomerization and subsequent autophosphorylation to induce downstream signaling. This N-terminal luminal domain (NLD) is conserved among mammals, *C.elegans*, and yeast (133). Autophosphorylation is essential for initiation of the PERK pathway. Su et al. (134) reported that more than one tyrosine residue could be phosphorylated by PERK's tyrosine kinase activity *in vitro* and *in vivo*. They further suggested that Tyr-615 is crucial for this autophosphorylation since mutation of this amino acid impaired the expression of ATF4 which is a downstream target of the PERK pathway.

Protein synthesis inhibition/ATF4 expression

In mammalian cells, the phosphorylation of eIF2 α by PERK induces protein synthesis inhibition to relieve the overloading of misfolded proteins in the ER during ER stress. PERK phosphorylates the α subunit of eIF2 α at serine51 (132, 135). Phosphorylated eIF2 α inhibits eIF2 β which is the guanine exchange factor for the eIF2 complex. This decreases the recycling of the 43S initiation complex and causes a decrease in translation initiation of mRNA and protein synthesis inhibition (136). Cyclin D1 is one of the targets of protein

synthesis inhibition during ER stress. When mammalian cells go through the G1 phase, type D cyclins associate with CDK (cyclin-dependent kinase) 4 or CDK6 to activate cyclin E- and A-dependent kinase CDK2 (137). Therefore, ER stress-induced loss of cyclin D1 inhibits CDK2 and causes cell cycle arrest in G1 phase (138). This is one of the important physiologic markers of ER stress.

eIF2 α phosphorylation inhibits general protein synthesis. However, studies (139-141) have shown that translation of certain target proteins will be up-regulated as a result of this phosphorylation. These mRNAs are not efficiently translated under normal conditions, but when eIF2 α gets phosphorylated under stress, the 40S scanning ribosomal subunit can efficiently recognize the AUG codons on the upstream open reading frame (uORF) within the 5' untranslated region (UTR) of these mRNAs. ATF4 is one such mRNA. ER stress can induce the expression of ATF4 through the phosphorylation of eIF2 α . ATF4 then acts as a transcription factor to induce downstream genes, such as CHOP, GADD34 (growth arrest and DNA damage-inducible gene 34) (139, 142), and ATF3 (143).

Nrf2

Nrf2 is another direct substrate of PERK (144). Normally, Nrf2 is found in the cytoplasmic complex and associates with Keap1, an actin-binding protein. Under stress, phospho-PERK phosphorylates Nrf2 and causes it to dissociate from Keap1 (145). After this dissociation, Nrf2 is imported to the nucleus where it forms heterodimers with ATF4 (146) or small Maf proteins, which are also transcription factors (147-148). These complexes activate the transcription of genes including phase II detoxifying enzymes through the ARE (antioxidant response element) as well as antiapoptotic genes to promote cell survival (146, 148-149). Cullinan et al. (144) also demonstrated that ER

stress-induced apoptosis was increased in the absence of Nrf2.

Regulation of the PERK pathway

It has been shown that p58^{IPK} containing an ERSE (ER stress element) in its promoter region can interact with PERK and negatively regulate eIF2 α phosphorylation (113, 150). PERK activation requires BiP dissociation. However, since BiP is highly expressed during ER stress, the BiP/PERK complex may re-associate and negatively regulate PERK activation (106, 151). Moreover, GADD34 which is a downstream target of the PERK pathway can form a complex with the catalytic subunit of protein phosphatase 1 (PP1 α). This complex acts as a negative-feedback loop to dephosphorylate eIF2 α and down-regulate the PERK pathway to restore protein synthesis in the late stage of ER stress (152-153).

Objectives of the thesis

Parikh et al. (154) have shown that in yeast, ricin inhibits UPR induced by tunicamycin and DTT. In this study, yeast were transformed with wild-type RTA or an active site mutant (E177K) of RTA. UPR induction was determined using a UPRE-driven *lacZ* reporter assay and *Hac1* mRNA splicing. They found that wild-type RTA could inhibit tunicamycin and DTT-induced β -gal expression and *HAC1* mRNA splicing. Furthermore, the induction of *KAR2*, the homolog of *BiP*, and *DER1*, an ERAD gene, were inhibited. Therefore, the goals of the present study were to determine (1) if RTA inhibits the UPR in mammalian cells; (2) if this effect is due to RTA-induced protein synthesis inhibition; and (3) if ER stress plays a role in RTA-induced cytotoxicity.

Chapter 2

Ricin-A-chain (RTA) inhibits the unfolded protein response (UPR) in mammalian cells

Introduction

Ricin is a glycosylated type II ribosome-inactivating protein (RIP) of 64 kDa. It is a byproduct of oil extraction from the castor bean plant (*Ricinus communis*) which originates from Asia and Africa. Due to its ease of isolation and extreme toxicity it has been classified by the Center for Disease Control as a category B select agent. It is composed of two polypeptide chains linked by disulfide bonds (5). Ricin-A-chain (RTA) is the enzymatic component of ricin while ricin-B-chain (RTB) contains galactose-binding sites that facilitate entry of the holotoxin into the cell via clathrin-dependent endocytosis and uptake into endosomes (9). After entry into the cell, ricin undergoes retrograde translocation to the endoplasmic reticulum (ER), where the disulfide bond between the two subunits is reductively cleaved to release RTA. RTA interacts with negatively-charged ER membrane lipids which causes its partial unfolding (25) and subsequent transport to the cytosol via the Sec61 channel. In the cytosol, RTA targets the 28S rRNA of the 60S ribosomal subunit. The N-glycosidase activity of RTA depurinates the adenine (A4324) on the exposed loop, the sarcin-ricin loop, of the 28S rRNA (6). The targeted sequence of the sarcin-ricin loop (AGUACGAGAGGAAC) is highly conserved between eukaryotes and prokaryotes and is essential for the binding of translation elongation factors (29). The RTA-modified rRNA has low affinity for elongation factor binding which results in protein synthesis inhibition (30).

The ER is an organelle that functions in calcium homeostasis, secretory and membrane protein synthesis, post-translational protein modification, and biosynthesis of lipid and sterols. Stresses that alter the normal ER environment reduce the folding capacity of the ER, resulting in the accumulation and aggregation of unfolded proteins - a

condition referred to as ER stress (51-52). Transmembrane receptors in the ER detect the onset of ER stress and activate a signaling cascade referred to as the unfolded protein response (UPR) to restore normal ER function. Therefore, the UPR is a prosurvival response that serves to restore ER homeostasis. However, if the stress is prolonged, or the adaptation fails, apoptotic cell death ensues. In mammalian cells, UPR involves activation of three main signal transducers: IRE1, ATF6, and PERK.

In yeast, RTA expression inhibits ER stress induced by tunicamycin (Tm) or dithiothreitol (DTT) (154). This was shown by inhibition of Tm or DDT-induced splicing of *HAC1* mRNA, the yeast homologue of XBP1 which is downstream of IRE1. They also found that wild-type RTA could inhibit the induction of *KAR2*, the homolog of the mammalian *Bip* gene and *DER1*, a gene that functions in ER-associated degradation (ERAD), a process by which misfolded proteins are directed to the lysosome for degradation. Here, we treated cells with RTA in addition to UPR- inducing reagents to determine if RTA would have a similar effect in mammalian cells. We were also interested in determining if this inhibition would affect ricin-induced cytotoxicity

Materials and Methods

Reagents

RTA, thapsigargin (Tg), Tm, dimethyl sulfoxide (DMSO), and RTA were purchased from Sigma-Aldrich. DTT was obtained from AnaSpec. Inc. Cell culture media were from Invitrogen and fetal bovine serum was purchased from Atlanta Biologicals.

Cell Culture

The human cervical cancer cell line (HeLa) was kindly provided by Dr. Tom O'Brig (University of Virginia, Charlottesville, VA) and was maintained as previously described (33). The bovine mammary epithelial cell (MAC-T) was established by immortalization with Simian virus 40 large T antigen (155) and was maintained as previously described (156). For experiments, cells were plated on 60 mm tissue culture plates in complete media containing serum and grown to confluence, washed twice with phosphate buffered saline (PBS) and then changed to serum-free media contained 0.2% bovine serum albumin (BSA) and 30 nM sodium selenite for 2 hours. After the serum-free wash, cells were incubated in serum-free media with treatments for various times as indicated in figure legends. Cells were lysed in lysis buffer for protein analysis as previously described (156) or Trizol (Invitrogen) for RNA analysis according to the manufacturer's recommendations.

Western Blotting

Total protein concentration was measured by Bradford protein assay (Bio-Rad Laboratories). Proteins were separated by SDS-PAGE on 8% gels. The proteins were transferred to 0.45 μ m PVDF membranes (Millipore) and Nitrocellulose membrane (Bio-Rad). Membranes were blocked in tris buffered saline (TBS) with 0.1% Tween-20 (TBST) in 5% skim milk for one hour at room temperature and incubated in primary antibodies overnight at 4°C. After incubation, the membranes were washed three times with TBST for 10 min each and incubated with secondary antibodies conjugated with the appropriate secondary antibody conjugated to horseradish peroxidase (anti-rabbit IgG from GE; anti-mouse IgG from Vector Labs; anti-goat IgG from Santa Cruz) for 1 h at room temperature and then washed three times with TBST. The peroxidase activity was

detected by enhanced chemiluminescence substrate (ECL) from Pierce. Total-eIF2 α antibodies were purchased from Santa Cruz; p-eIF2 α , total-IRE1, cleaved Caspase 3, total and cleaved Caspase 7 antibodies were obtained from Cell Signaling Technology; p-IRE1 was from Novus Biological.

RT-PCR assay to detect XBP1 splicing

Total RNA was isolated by the Qiagen RNeasy kit. The isolated RNA concentration was measured by the NanoDrop™ 1000 Spectrophotometer and RNA integrity was examined by agarose gel electrophoresis. To assess XBP1 splicing, total RNA (2 μ g) was reverse transcribed using the High Capacity cDNA Reverse Transcription Kit (Applied Biosystems). The PCR primers were: human F 5'-CCT TGT AGT TGA GAA CCA GG-3'; R 5'-GGG GCT TGG TAT ATA TGT GG-3'; and bovine F 5'-CCT TGT AGT TGA GAA TCA GG-3'; R 5'-GGG GCT TTG TAT ACG TGA-3' and were obtained from Sigma-Aldrich (Figure 3). 10X PCR gold buffer, MgCl₂, dNTP, and Ampli-Taq Gold were all purchased from Applied Biosystems. PCR was performed with the following conditions: initial denaturation step, 95 °C for 10 mins, and repeating 35 cycles of 95 °C for 1 min, 50 °C for 1 min, and 72 °C for 1 min, and then final extension step, 72 °C for 10 min. The amplified PCR products were separated by argarose gel electrophoresis on 3% gels and visualized with ethidium bromide.

Quantitative(q) RT-PCR

For qRT-PCR, primers were as follows: Spliced XBP1: human F 5'-TGC TGA GTC CGC AGC AGG-3'; R 5'-CGC CAG AAT CCA TGG GGA GA-3'; bovine F 5'-TGC TGA GTC CGC AGC AGG-3'; R 5'-CAT CAG AGT CCA TGG GGA GA-3'. Total XBP1:

human F 5'-GCA AGC GAC AGC GCC T-3'; R 5'-TTT TCA GTT TCC TCC TCA GCG;
 bovine F 5'-GCA AGC GAC AGC GCC T; R 5'-TTT TCA GTT TCC TCC GCA GCG-3'
 (Figure 4). BIP: human F 5'-TGT TCA ACC AAT TAT CAG CAA ACT C-3'; R 5'-TTC
 TGC TGT ATC CTC TTC ACC AGT-3'; bovine F 5'-TGG AGA AGA CTT TGA CCA
 GCG TGT-3'; R 5'-ACA GCT CTG TTG TCC TTC CGA ACA-3'. Human actin: 5'-AAT
 GTG GCC GAG GAC TTT GAT TGC-3'; R 5'-AGG ATG GCA AGG GAC TTC CTG
 TAA-3'. Bovine cyclophilin: 5'-GAG CAC TGG ACA GAA AGG ATT TGG-3'; R
 5'-TGA AGT CAC CAG CCT GGC ACA TAA-3'. Each primer set was validated by
 generating a standard curve from a pool of cDNA with serial dilutions ranging from 1:2 to
 1:20,000.

The expression of target genes in individual samples was measured using an Applied Biosystems 7300 Real-time PCR system. A dilution of cDNA (ranging from 1:4 to 1:20 for different genes)-was amplified in a total reaction volume of 20 μ l that included 250 nM forward and reverse primers (5 pmole each), 10 μ l of Power SybrGreen PCR MasterMix (Applied Biosystems. For each experimental sample, values were calculated relative to untreated control samples using the $2^{-\Delta\Delta CT}$ method with actin or cyclophilin as the housekeeping gene.

Statistical analysis

Data were analyzed by one-way ANOVA with Newman-Keuls post-tests or paired t-test using GraphPad Prism 5 Software and SAS Version 9.2 Software.

Results

RTA inhibits XBP1 splicing in mammalian cells.

The previous study of Parikh et al. (154) showed that in yeast, RTA inhibited Tm-induced Hac1 mRNA splicing, which is downstream of IRE1. We therefore investigated whether RTA would have a similar effect on XBP-1, the mammalian homologue of Hac1. In our previous paper (33), we reported that the non-transformed mammary epithelial cell line MAC-T was extremely sensitive to RTA in terms of depurination, protein synthesis inhibition, and apoptosis. Therefore we chose this mammalian cell line as a model to examine the effect of RTA on XBP-1 splicing. As shown in Fig. 4A, only the unspliced form of XBP-1 was present in cells treated with either 0.1 or 1.0 $\mu\text{g/ml}$ RTA alone, indicating that RTA did not affect XBP-1 splicing. As expected, treatment with Tm, which blocks N-linked glycosylation to induce ER stress, caused XBP1 mRNA splicing in MAC-T cells as shown by the decrease in the upper unspliced form and appearance of the smaller spliced form of XBP1. Using a qRT-PCR assay, 0.1 and 1.0 $\mu\text{g/ml}$ RTA was found to inhibit Tm-induced XBP-1 splicing by 50 to 87%, respectively (Fig. 4B). We also measured total XBP1 mRNA by qRT-PCR to determine if this inhibition was related to inhibition of total XBP1 mRNA in the presence of RTA (Fig. 4C). Total XBP1 mRNA expression was not different between cells treated with Tm alone and those treated with Tm and 0.1 $\mu\text{g/ml}$ RTA, suggesting that at this concentration of RTA, total XBP1 levels were not inhibited. However, the higher dose of RTA inhibited total XBP1 in Tm-treated cells by approximately 50%.

In order to determine if the inhibition of XBP-1 mRNA splicing by RTA was cell type specific, the experiments were repeated in HeLa cells, a human cervical carcinoma cell line,

which are also responsive to RTA in our previous work (33). Like MAC-T cells, RTA alone could not induce XBP1 mRNA splicing in HeLa cells (Fig. 2). As shown in Fig. 5A and 5B, at 4 hour, 1 μ g/ml RTA inhibited Tm-induced XBP1 mRNA splicing by 35%. As shown in Figure 5A, inhibition was also observed increased with longer treatment. This inhibition at 4 h was not due to a decrease in total XBP1 mRNA since RTA induced more total XBP1 expression compared to Tm treated cells (Fig. 5C).

To determine if RTA could inhibit XBP1 splicing in response to other ER stress-inducing agents, HeLa cells were treated with thapsigargin (Tg), which causes ER stress by disrupting calcium concentrations, and DTT, which reduces disulfide bonds of proteins. In contrast to Tm, RTA could not inhibit Tg and DTT induced XBP1 mRNA splicing at 4 h as determined by both XBP1 splicing assay (Fig.6A, B) and qRT-PCR (Fig. 6C-F). Similar results were observed with MAC-T cells for both DTT and Tg using the semi-quantitative XBP1 splicing assay (data not shown). Since HeLa cells are less sensitive to RTA than MAC-T cells, longer treatment intervals were examined. When cells were treated longer, RTA could partially inhibit this mRNA splicing. As shown in Fig. 6A, the intensity of the spliced form of XBP1 mRNA was not different between Tm- or DTT- treated cells with or without RTA at 6 or 8 h. However, unspliced XBP1 appeared to be increased. Unfortunately, the qPCR data for 6 and 8 h treatment were not available because of the inconsistency of housekeeping genes with longer exposure to RTA.

RTA inhibits Tm-induced phosphorylation of IRE1

Since RTA inhibited ER stress-induced XBP1 mRNA splicing, we looked upstream of XBP1 at IRE1 phosphorylation. As shown in Fig. 7, Tm, Tg, and DTT each induced IRE1 phosphorylation at least 3-fold, with the largest induction observed with DTT. Similar to

the results of the XBP1 mRNA splicing assay, RTA alone could not induce IRE1 phosphorylation. With treatment of 1 $\mu\text{g/ml}$ RTA, *Tm-induced* IRE1 phosphorylation was decreased approximately 45% (Fig. 7B) while Tg and DTT-induced phosphorylation of IRE1 were not altered. Total IRE1 protein levels changed by the DTT treatment was observed in two of our experiments.

RTA inhibits the DTT-induced phosphorylation of eIF2 α

PERK, another arm of UPR, is not only structurally similar to IRE1 but also shares a similar mechanism of activation during induction of ER stress. Thus, we also wanted to determine if RTA could affect the PERK pathway. To determine if the PERK pathway was activated, western blotting of phospho-eIF2 α was performed. eIF2 α is a direct substrate of phospho-PERK, the active form of PERK. As shown in Fig. 8, RTA alone could not induce eIF2 α phosphorylation at 4 h treatment. eIF2 α phosphorylation was induced 2- to 4-fold compared to untreated controls by exposure to Tm, Tg, or DTT. When HeLa cells were treated with these UPR inducing reagents in the presence of RTA, DTT-induced eIF2 α phosphorylation was dramatically inhibited by approximately 80% relative to cells treated with DTT. However, RTA could not inhibit the Tm- and Tg-induced eIF2 α phosphorylation. Interestingly, RTA increased Tg-induced eIF2 α phosphorylation although this effect was not statistically significant.

RTA inhibits Tm-induced BiP mRNA expression

Since BiP is downstream of both the IRE1 and PERK pathways and is also a key marker of ER stress, we determined if BiP mRNA could be regulated by RTA as well. RTA alone did not induce BiP mRNA expression in either cell line. As shown in Fig. 9A

and C, BiP mRNA was induced by Tm approximately 6 fold in HeLa cells and over 20-fold in MAC-T cells. RTA inhibited Tm-induced BiP mRNA expression approximately 47% compared to cells treated with Tm alone (Fig. 9B) while Tm-induced Bip mRNA expression was decreased approximately 28% to 36% by 0.1 $\mu\text{g/ml}$ and 1 $\mu\text{g/ml}$ RTA, respectively (Fig. 9D). While Tg induced Bip mRNA levels 10- to 14- fold in HeLa cells (Fig. 10A), this effect was not affected by RTA (Fig. 10B). DTT had no effect on Bip mRNA levels, therefore it was not surprises that RTA had no effect (Fig. 11).

Inhibition of ER stress sensitizes cells to RTA-induced cytotoxicity

Activation of the UPR pathway represents a survival response that allows the cell to recover homeostasis after an ER overload. Since RTA inhibited both the IRE1 and PERK pathways induced by Tm and DTT, respectively, we were interested in determining if RTA was more cytotoxic in the absence of the UPR-survival pathway. We have previously reported that RTA activates cleavage of caspase-3 and -7 in MAC-T cells (33). Therefore, to examine apoptosis, immunoblot analysis of cleaved caspase-3 and -7 was examined. As shown in Fig12, caspase-3 and -7 were not cleaved with UPR-inducing reagents alone while cleavage was observed in the presence of RTA alone. However, when cells were treated with Tm and DTT in combination with *RTA*, caspase cleavage was clearly augmented. However, Tg had no effect on caspase cleavage by RTA. These data indicate inhibition of UPR by RTA could make cells more vulnerable to cell death.

Discussion

The overall goal of this study was to determine if RTA affects ER stress in mammalian

cells. Since ricin uses retrograde translocation to enter the cell and arrive at the ribosome (8), it has been proposed that RTA may act similar to unfolded proteins to activate UPR. However, in the present study, RTA did not induce UPR between 4 to 6 hr in MAC-T or HeLa cells. We have also confirmed this result using ricin holoenzyme (data not shown). We have previously reported that RTA induces apoptosis in both cell lines within this timeframe, as well as depurination and protein synthesis inhibition in MAC-T cells (33). This agrees with work in yeast, which showed that RTA alone could not induce UPR. Interestingly, others have reported that Shiga toxin, which shares a similar retrograde transport pathway with RTA, induces the UPR (157-159).

While RTA alone did not induce UPR, it did inhibit UPR induced by ER-stress compounds. In the present study, we found that RTA inhibited XBP1 mRNA splicing induced by Tm in both HeLa and MAC-T cells, indicating that this inhibition was not cell-type or species specific. This result agrees with the study of Parikh et al. (154) who showed that RTA inhibited Tm-induced *Hac 1* mRNA splicing in yeast, which is the yeast homolog of mammalian XBP1.

Since XBP1 splicing is induced by activation of the signaling molecule IRE1, we investigated IRE1 phosphorylation. We found that RTA also inhibited IRE1 autophosphorylation during ER stress. We could not determine if this inhibition of IRE1 phosphorylation also occurred in MAC-T cells since the IRE1 antibody did not recognize the bovine protein. It has been proposed that ricin can associate with other RNA substrates in addition to ribosomal RNA (160). Specifically, Parikh et al. (154) suggested that *Hac1* mRNA might be a substrate for RTA, which might bind *Hac1* mRNA and somehow inhibit splicing. However, the results of the present study show that RTA not

only inhibited XBP1 mRNA splicing during ER stress, but also inhibited autophosphorylation of IRE1 which is upstream of the splicing event. This suggests that RTA does not directly associate with XBP1 mRNA to inhibit splicing, but inhibits XBP1 mRNA splicing by inhibiting activation of IRE1.

Interestingly, the ability of RTA to inhibit IRE1 phosphorylation and XBP-1 splicing was not observed when ER stress was induced with DTT. However, RTA did dramatically inhibit the PERK arm of UPR, as evidenced by its ability to decrease DTT-induced eIF2a phosphorylation. Interestingly, RTA did not inhibit Tm-induced eIF2a phosphorylation. During UPR, unfolded proteins accumulate in the ER lumen. This causes the chaperone protein BiP to dissociate from ER-membrane associated IRE1 and PERK. One potential mechanism by which RTA could inhibit phosphorylation of these two signaling molecules would be to reduce general protein synthesis so that BiP fails to dissociate from IRE1 and PERK, which would prevent oligomerization and subsequent phosphorylation. However, if this was the mechanism, RTA would be expected to inhibit both signaling pathways in response to either Tm or DTT. The finding that a different branch of UPR was inhibited by RTA in Tm-induced ER stress compared to DTT-induced ER stress suggests that RTA is not using a general mechanism involving protein synthesis inhibition to inhibit UPR.

While the present data suggest specific mechanisms of action for inhibition of Tm-induced UPR relative to DTT-induced UPR, the effect could be elicited from either the luminal or the cytosolic side of the ER. Parikh et al. (154) showed that both pre-RTA, which contains the ER localization sequence, and mature RTA, which lacks this sequence, inhibit Tm-induced UPR in yeast. Since mature RTA does not enter the ER, these authors suggested that RTA inhibits UPR from the cytosolic side of the ER and not the luminal side.

Our data support this hypothesis since both IRE1 and PERK phosphorylation occur on the cytosolic side of the ER. However, since RTA inhibited both the IRE1 and PERK pathways induced by Tm and DTT, respectively, and the sequence of their luminal domains and mechanism of activating UPR are highly conserved, it is also possible that the UPR inhibition by RTA is located in the ER lumen. This needs to be further determined by observing if RTA would affect IRE1 and PERK oligomerization or dissociation of BiP.

In contrast to its effects on Tm- and DTT-induced UPR, RTA did not inhibit any of the Tg-induced responses in this study. Calcium concentration is essential for transport of proteins across the ER membrane (161), including translocation of RTA into the cytosol from the ER. This is due to the fact that translocation requires chaperone proteins, such as BiP and calnexin, which are calcium-dependent. One possible explanation for the lack of an RTA inhibitory effect on Tg-induced UPR is that treating with Tg would disrupt the calcium concentration in the ER and decrease the translocation of RTA from the ER to the cytosol (162). Moreover, this explanation would provide additional support for the idea that the RTA inhibition occurs on the cytosolic side of the ER.

In general, the UPR is a survival response that facilitates the restoration of homeostasis by removing misfolded proteins. However, if the cells cannot recover from this stress, the UPR will remove cells by apoptosis to protect the healthy cells. It was originally thought that the cytotoxicity of ricin is due to its ability to inhibit protein synthesis. However, recent work suggests that protein synthesis inhibition caused by ribosome depurination in response to ricin is not sufficient to induce apoptosis (32-33). In the present study, RTA induced caspase 3 and 7 cleavage in MAC-T and HeLa cells within 4 h. When cells were treated with RTA in combination with Tm or DTT, the cleavage of

caspase-3 and -7 were greater than what was observed in both cell lines in response to RTA, Tm, or DTT alone. BiP is a downstream target gene of several transcription factors induced during ER stress. It is well-accepted that BiP is an ER chaperone that is essential for facilitating cell recovery from ER stress. Tm-induced BiP mRNA induction was decreased by RTA in both cell lines. Thus, the inhibition of BiP induction would prevent the cells from relieving stress, resulting in apoptosis (163-165). These data fit with the data indicating that RTA inhibits IRE1 phosphorylation and XBP1 splicing, since BiP is downstream of this pathway. Therefore, RTA may ultimately inhibit the UPR survival response in part by decreasing the BiP response.

Interestingly, DTT did not induce BiP mRNA expression in the present study. This may be because HeLa cells were only treated with DTT during the last 30 min of RTA treatment because longer exposure to DTT is toxic to the cells. This might be too short to see the induction of BiP. However, the finding that caspase cleavage was still greater with RTA and DTT treatment in the absence of BiP induction suggests that inhibition of other components of the UPR pathway were sufficient to enhance the apoptotic effect of RTA.

In conclusion, we show here that RTA can inhibit UPR by inhibiting the IRE1 and PERK pathways. This inhibition also increased the cytotoxicity of RTA and made the cells more sensitive to ER stress. It has been suggested that ER stress could be related to various diseases, especially cancer (78, 166-167). Ricin also has been studied as an immuotoxin for targeting cancer cells (37-39). The ability of RTA to enhance its own cytotoxicity by inhibiting UPR represents another mode of action that may be important in the treatment of several diseases.

Figures

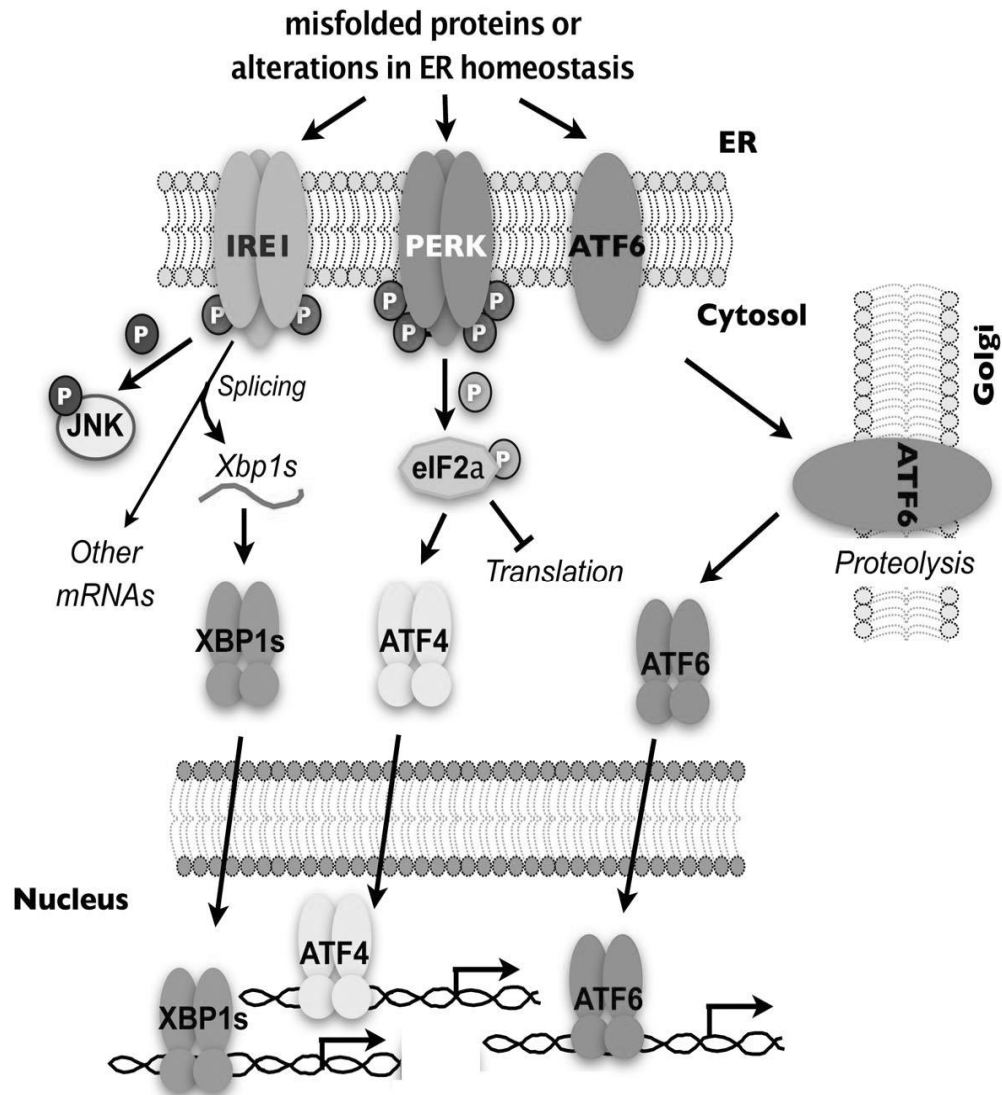


Figure 1. Signaling pathways of UPR.

During ER stress, three pathways will be activated: IRE1, PERK, and ATF6. The ultimate goal of these pathways is to help cells recover from ER stress. However, if the stress is prolonged, these pathways will induce apoptosis. Adapted from Qi's Lab, Division of Nutritional Sciences, College of Human Ecology, Cornell University, NY. (<http://www.human.cornell.edu/che/DNS/qilab/research.cfm>)

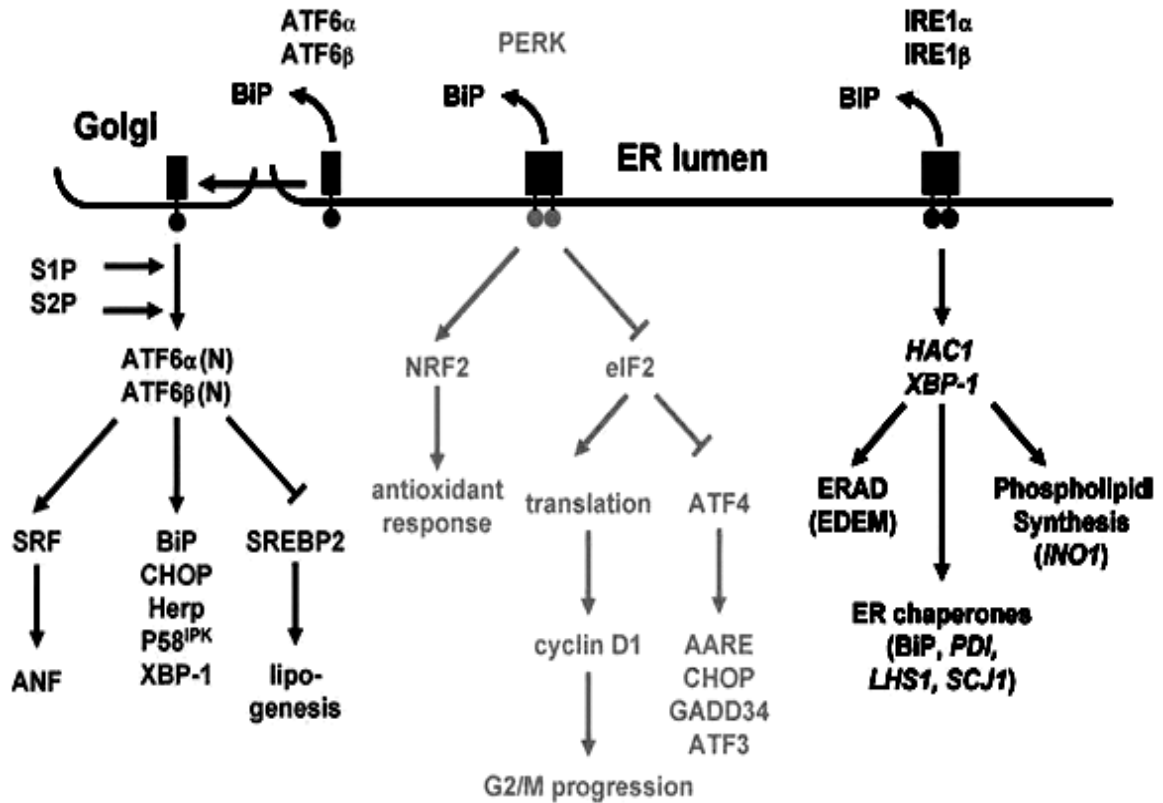


Figure 2. Downstream signaling of UPR pathway.

During ER stress, IRE1, PERK, and ATF6 are activated to induce various downstream signaling of unfolded protein response. Adapted from Schroder M and Kaufman RJ (168).

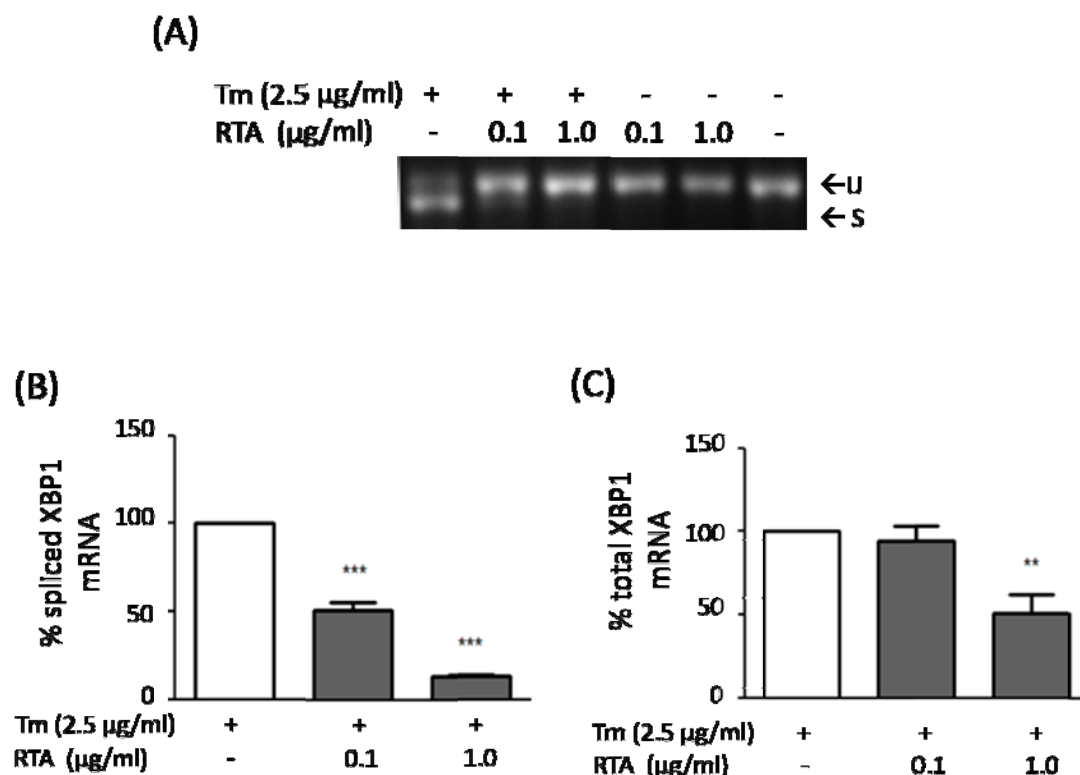


Figure 5 Exogenous RTA inhibits tunicamycin (Tm)-induced XBP1 splicing in MAC-T cells

Cells were serum-starved for 2 h prior to treatment \pm RTA and \pm Tm for 4 h. DMSO and glycerol served as vehicle controls. (A) Total RNA was isolated and analyzed by RT-PCR as described in Materials and Methods. The upper band (U) represents unspliced XBP1 while the lower band (S) represents the spliced form. Total RNA were also analyzed by qRT-PCR for (B) spliced XBP1 mRNA and (C) total XBP1 mRNA. Data were corrected for cyclophilin and presented relative to spliced XBP1 and total XBP1 in cells treated with Tm alone. Data were analyzed by one-way ANOVA with Newman-Keuls. *** $p < 0.001$ and ** $p < 0.01$ indicates different from Tm-treated cells. Bars represent mean \pm S.E. of four experiments.

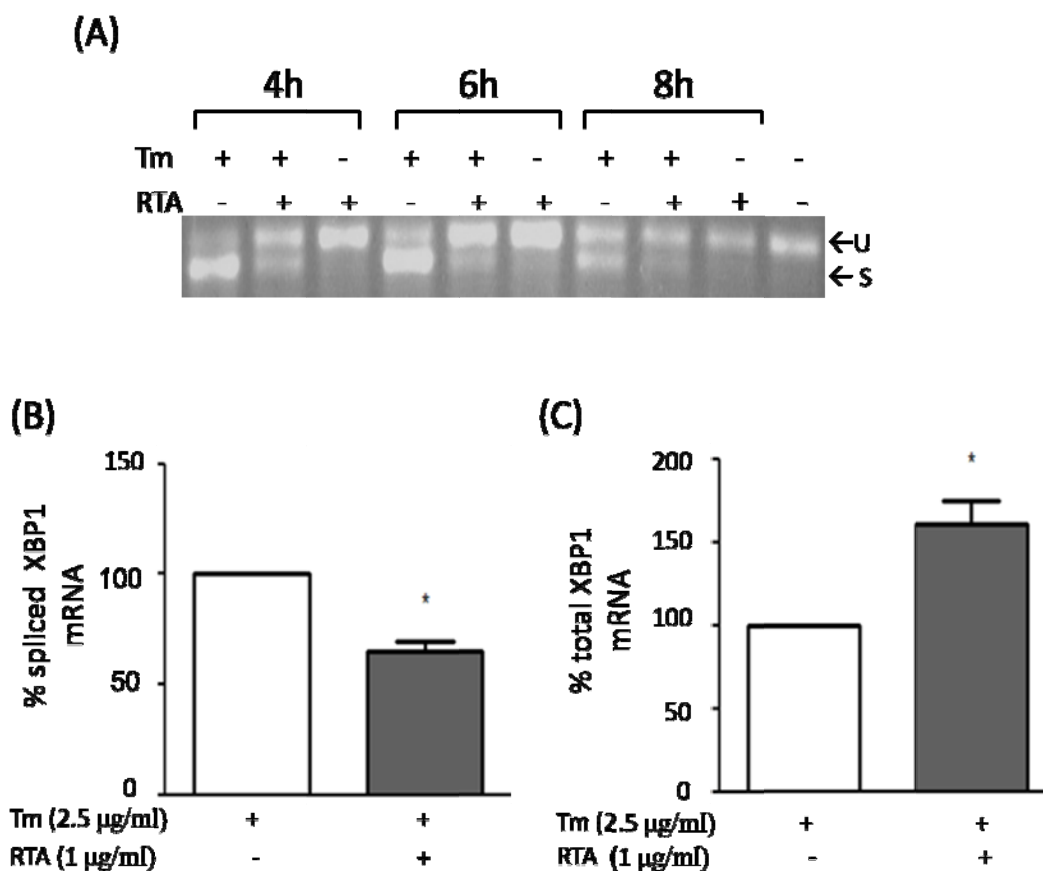


Figure 6. Exogenous RTA inhibits Tm-induced XBP1 splicing in HeLa cells

HeLa cells were serum-starved for 2 h prior to treatment \pm RTA (1 $\mu\text{g/ml}$) and \pm Tm (2.5 $\mu\text{g/ml}$). DMSO and glycerol served as vehicle controls. (A) Total RNA was isolated and analyzed by RT-PCR as described in Materials and Methods. The upper band (U) represents unspliced XBP1 while the lower band (S) represents the spliced form. Total RNA collected after 4 h of treatment was also analyzed by qRT-PCR for (B) spliced XBP1 mRNA and (C) total XBP1 mRNA. Data were corrected for cyclophilin and presented relative to spliced XBP1 and total XBP1 in cells treated with Tm alone. qRT-PCR data for the 6 and 8 h time points were not presented since a housekeeping gene that did not decrease with treatment was not identified. Data were analyzed by paired student's t-test. * $p < 0.05$ indicates different from Tm-treated cells. Bars represent mean \pm S.E. of four experiments.

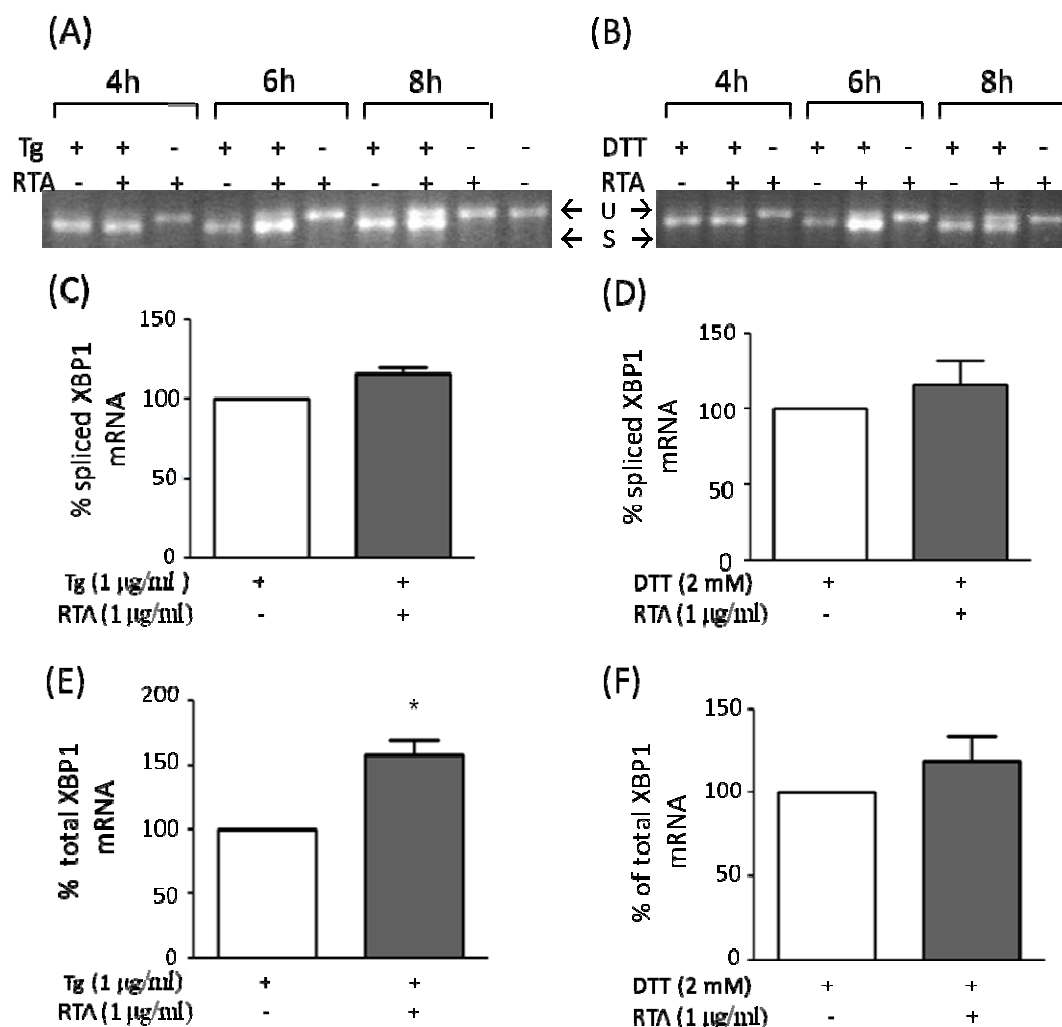


Figure 7. Effect of exogenous RTA on thapsigargin (Tg) and DTT-induced XBP1 splicing in HeLa cells

Cells were serum-starved for 2 h prior to treatment with RTA (1 $\mu\text{g/ml}$) \pm Tg (1 $\mu\text{g/ml}$) for the total treatment interval (A, C, E) or \pm RTA (1 $\mu\text{g/ml}$) with DTT (2 mM) added over the last 30 min of treatment (B, D, F). DMSO and glycerol served as vehicle controls. Total RNA was isolated and analyzed for XBP-1 by RT-PCR (A, B) as described in Materials and Methods. The upper band (U) represents unspliced XBP1 while the lower band (S) represents the spliced form. For the 4 h time point, spliced (C, D) and total (E, F) XBP1 mRNA were analyzed by qRT-PCR. Data were corrected for actin and presented relative to spliced XBP1 and total XBP1 in cells treated with Tg or DTT alone. qRT-PCR data for the 6 and 8 h time points were not presented since a housekeeping gene that did not decrease with treatment was not identified. Data were analyzed by paired student's t-test. * $p < 0.05$; indicates different from Tg alone. Bars represent mean \pm S.E. of four experiments.

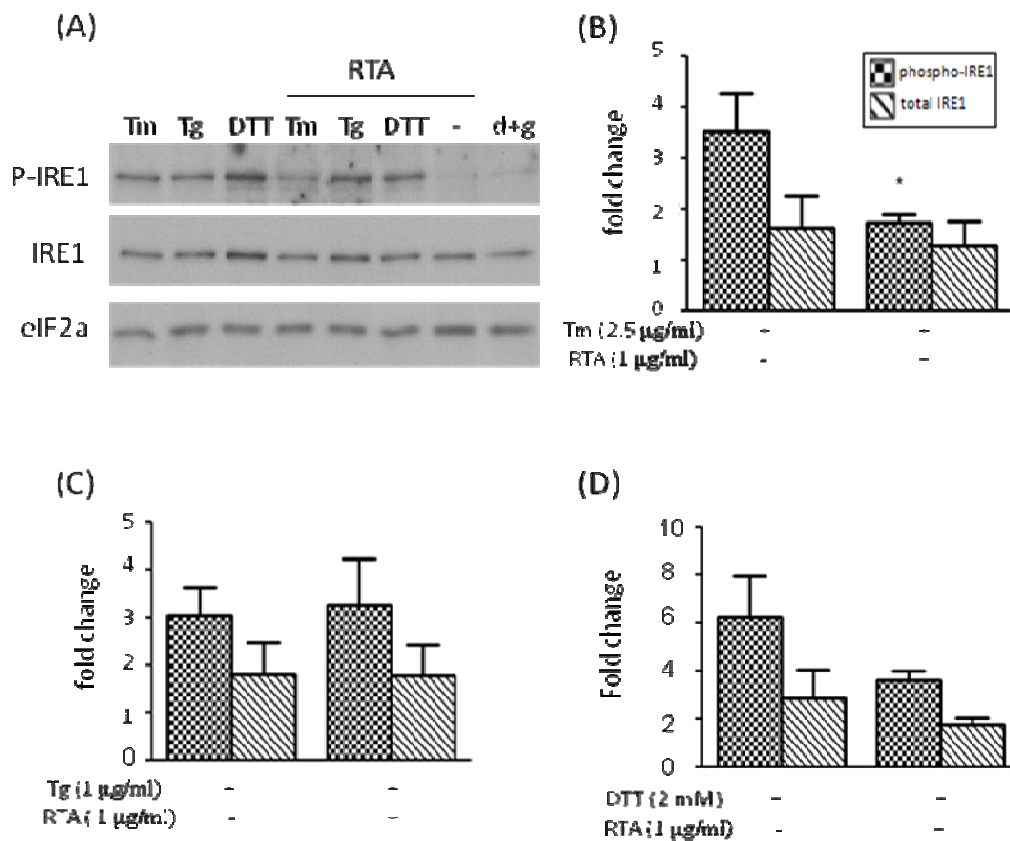


Figure 8. Exogenous RTA inhibits Tm-induced phosphorylation of IRE1 in HeLa cells

Cells were serum-starved for 2 h prior to treatment with RTA (1 μg/ml) ± Tm (2.5 μg/ml) or Tg (1 μg/ml) for 4 h or with RTA (1 μg/ml) for 4 h with DTT (2 mM) added over the last 30 min of treatment. DMSO (d) and glycerol (g) served as vehicle controls. Total cell lysate (50 μg) were separated by 8% SDS-PAGE, immunoblotted, and quantified by densitometry. A representative blot is shown in panel A. Data were analyzed by one-way ANOVA, * $p < 0.05$; indicates different from Tm alone. pIRE1 and total IRE1 expression were corrected for total eIF2 α . Bars represent mean \pm S.E. of three experiments.

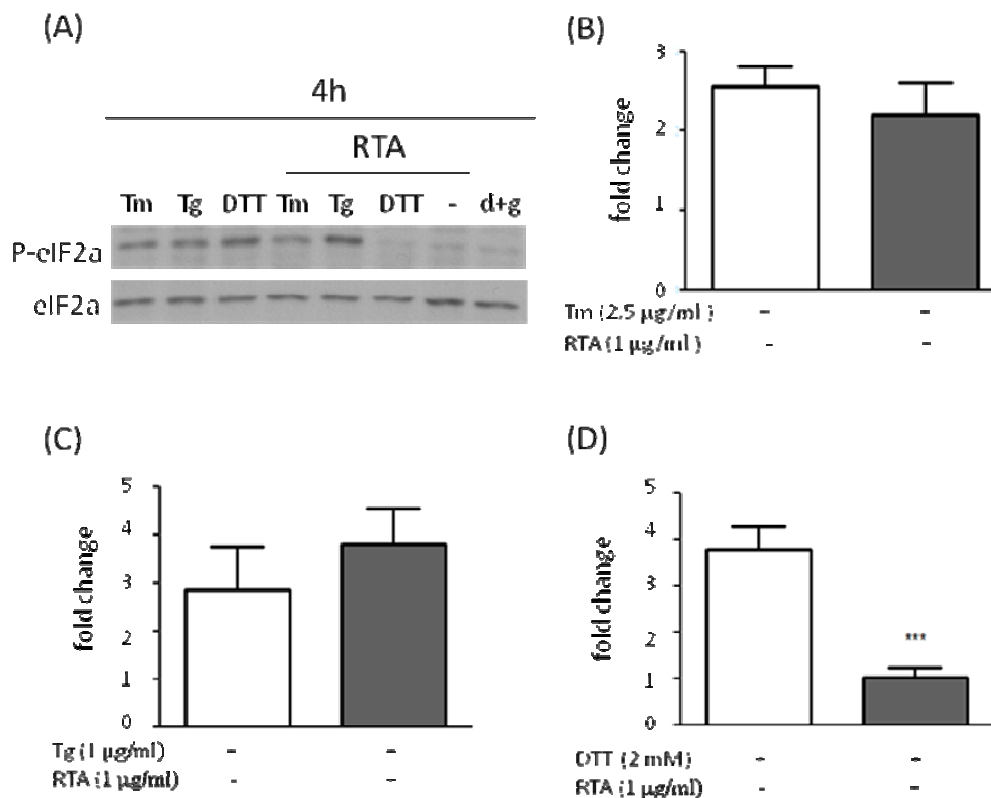


Figure 9. Exogenous RTA inhibits DTT-induced phosphorylation of eIF2 α in HeLa cells

Cells were serum-starved for 2 h prior to treatment with RTA (1 μg/ml) ± Tm (2.5 μg/ml) or Tg (1 μg/ml) for 4 h or with RTA (1 μg/ml) for 4 h with DTT (2 mM) added over the last 30 min of treatment. DMSO (d) and glycerol (g) served as vehicle controls. Total cell lysates (50 μg) were separated by 10% SDS-PAGE, immunoblotted, and quantified by densitometry. A representative blot is shown in Panel A. Data were analyzed by one-way ANOVA, *** $p < 0.001$ indicates different from DTT alone. p-eIF2 α expression was corrected for total eIF2 α . Bars represent mean \pm S.E. of three experiments.

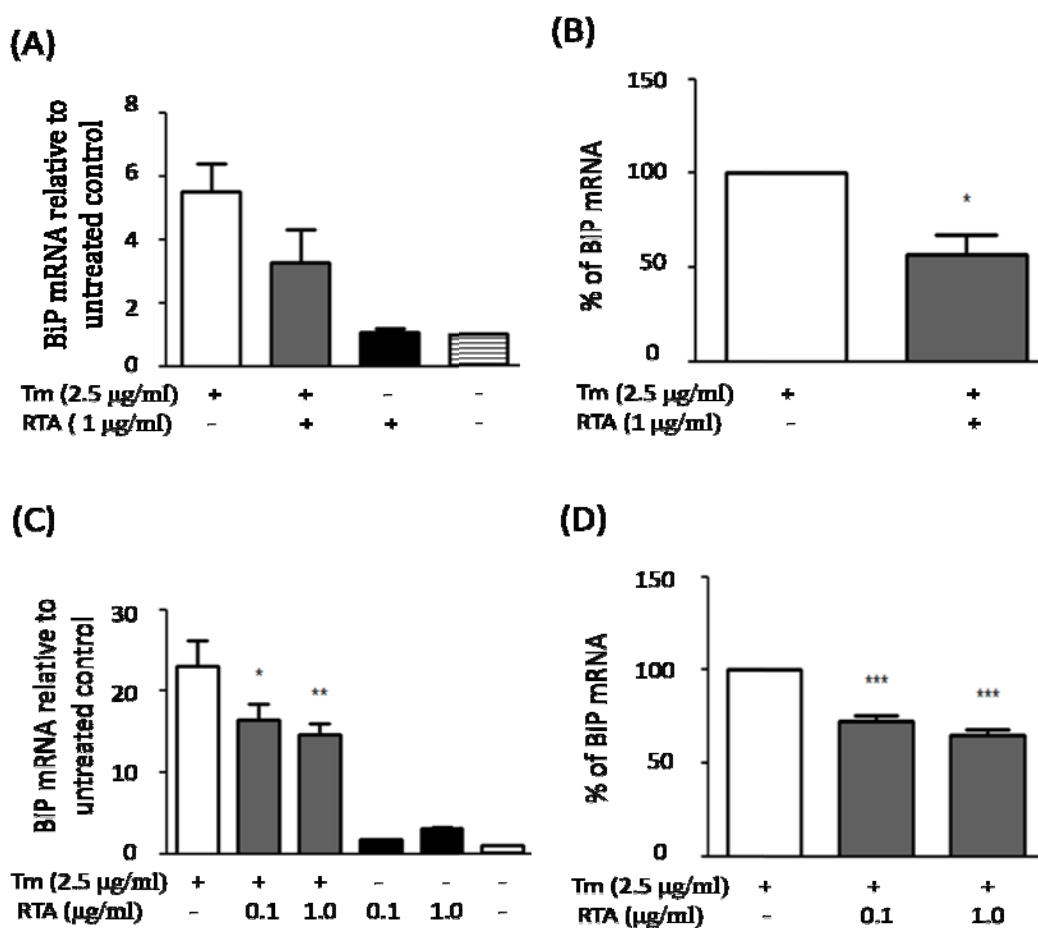


Figure 10. Exogenous RTA inhibits Tm-induced BiP mRNA expression in MAC-T and HeLa cells

Cells were serum-starved for 2 h prior to treatment with RTA \pm Tm (2.5 $\mu\text{g/ml}$) for 4 h. Total RNA was isolated and analyzed for BiP mRNA by qRT-PCR. (A, C) BiP mRNA levels relative to untreated vehicle controls in HeLa and MAC-T cells, respectively. (B, D) BiP mRNA levels expressed relative to HeLa or MAC-T cells, respectively, treated with Tm alone. Data were corrected for actin (HeLa) or cyclophilin (MAC-T), respectively, and were analyzed by one-way ANOVA with Newman-Keuls. * $P < 0.05$, ** $p < 0.01$, *** $p < 0.0001$; indicates different from Tm alone. Bars represent mean \pm S.E. of three experiments.

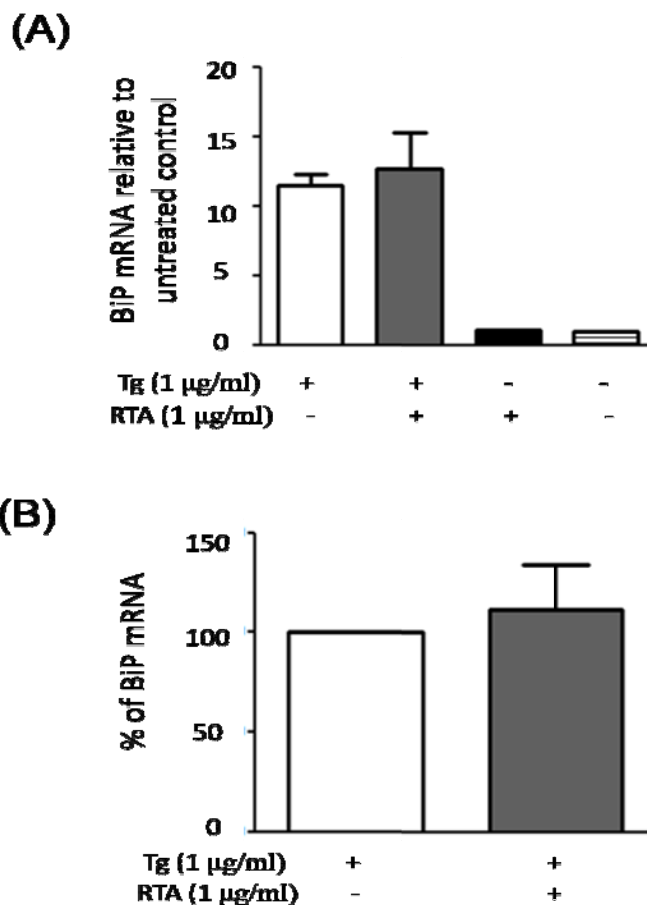


Figure 11. Exogenous RTA does not inhibit Tg-induced BiP mRNA expression in HeLa cells

Cells were serum-starved for 2 h prior to treatment with RTA \pm Tg for 4 h. Total RNA was isolated and analyzed for BiP mRNA by qRT-PCR. (A) BiP mRNA levels relative to untreated vehicle controls. (B) BiP mRNA levels expressed relative to HeLa cells treated with Tg alone. Data were corrected for actin and were analyzed by one-way ANOVA with Newman-Keuls. Bars represent mean \pm S.E. of four experiments

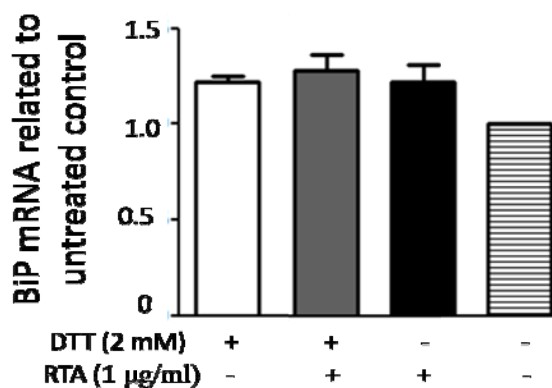
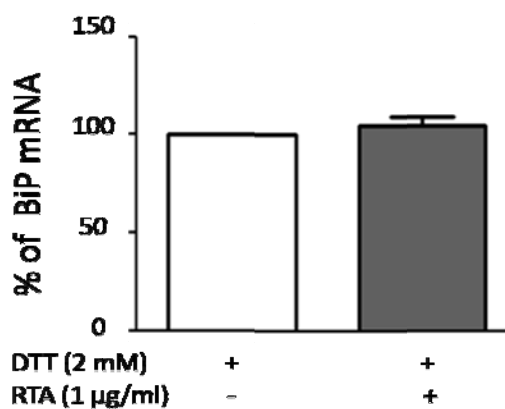
(A)**(B)**

Figure 12. DTT does not induce BiP mRNA in HeLa cells at 30 mins.

Cells were serum-starved for 2 h prior to treatment with RTA for 4 h. DTT was added over the last 30 min of RTA treatment. Total RNA was isolated and analyzed for BiP mRNA by qRT-PCR. (A) BiP mRNA levels relative to untreated vehicle controls. (B) BiP mRNA levels expressed relative to HeLa cells treated with DTT alone. Data were corrected for actin and were analyzed by one-way ANOVA with Newman-Keuls. Bars represent mean \pm S.E. of three experiments.

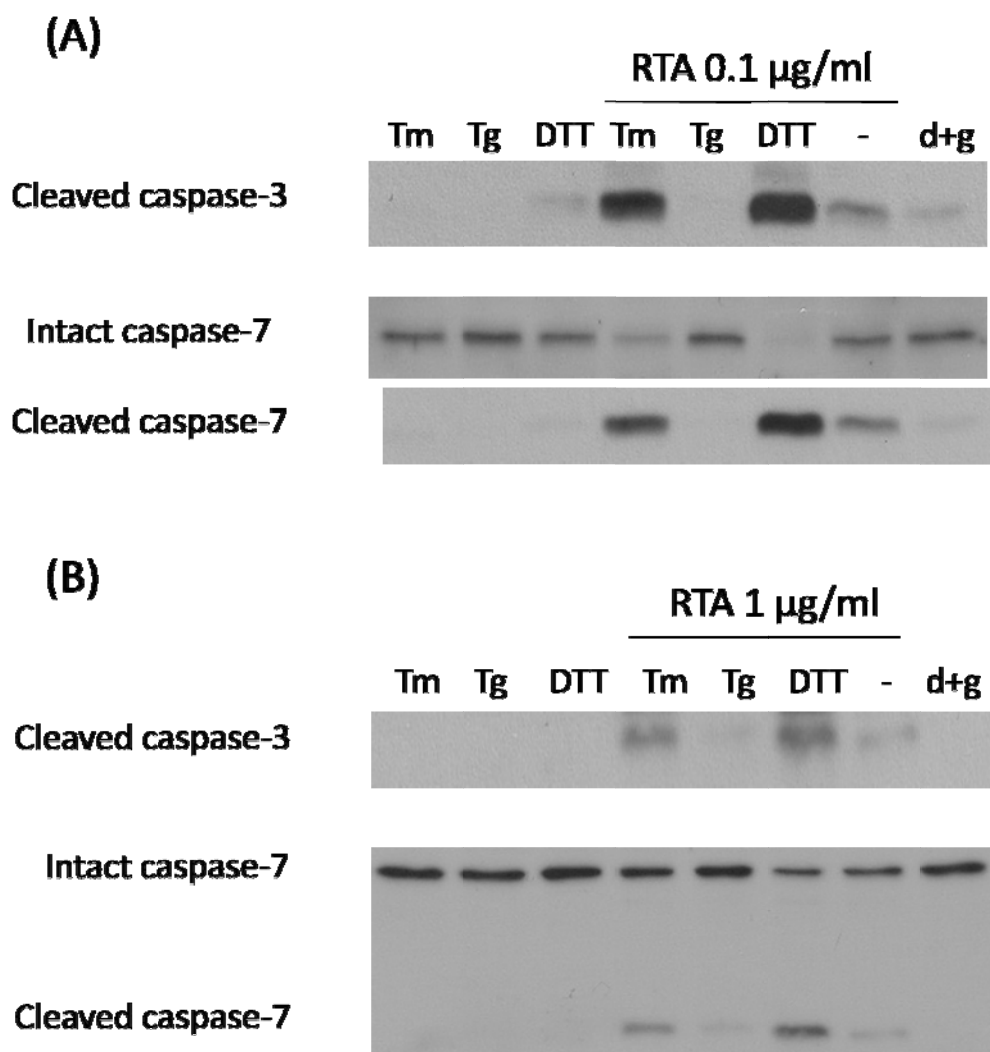


Figure 13. Caspase cleavage is enhanced in cells treated with both exogenous RTA and UPR-inducing agents

(A) MAC-T cells were serum-starved for 2 h prior to treatment with RTA and Tm (2.5 $\mu\text{g/ml}$), Tg (1 $\mu\text{g/ml}$) or DTT (2 mM) for 4 h. (B) HeLa cells were serum-starved for 2 h prior to treatment with RTA and Tm (2.5 $\mu\text{g/ml}$) or Tg (1 $\mu\text{g/ml}$) for 4 h or RTA for 4 hr with DTT (2 mM) added over the last 30 min of treatment. Total cell lysates (30 μg for MAC-T and 50 μg for HeLa) were separated by 15% SDS-PAGE and immunoblotted with cleaved caspase-3, total and cleaved caspase-7 antibodies.

Abbreviation List

ATF	activating transcription factor
DTT	dithiothreitol
EDEM	ER degradation-enhancer mannosidase-like alpha 1
eIF2 α	eukaryotic initiation factor 2 alpha
ER	endoplasmic reticulum
ERAD	ER-associated degradation
ERSE	ER stress element
GRP	glucose-regulated protein
HRD1	HMG-CoA reductase degradation
IRE1	inositol-requiring protein 1
PDI	protein disulfide isomerase
PERK	pancreatic ER kinase (PKR)-like ER kinase
RIP	Ribosome-inactivating protein
SERCA	Sarco ER calcium ATPase
Tg	thapsigargin
Tm	tunicamycin
TRAF2	TNF receptor-associated factor 2

UGGT	UDP-glucose: glycoprotein glucosyltransferase
XBP1	X-box binding protein 1

References

1. Rauber A, Heard J. Castor bean toxicity re-examined: a new perspective. *Vet Hum Toxicol.* 1985 Dec;27(6):498-502.
2. Balint GA. Ricin: the toxic protein of castor oil seeds. *Toxicology.* 1974 Mar;2(1):77-102.
3. Kumar O, Sugendran K, Vijayaraghavan R. Oxidative stress associated hepatic and renal toxicity induced by ricin in mice. *Toxicon.* 2003 Mar 1;41(3):333-8.
4. Audi J, Belson M, Patel M, Schier J, Osterloh J. Ricin poisoning: a comprehensive review. *JAMA.* 2005 Nov 9;294(18):2342-51.
5. Olsnes S, Pihl A. Different biological properties of the two constituent peptide chains of ricin, a toxic protein inhibiting protein synthesis. *Biochemistry.* 1973 Jul 31;12(16):3121-6.
6. Endo Y, Mitsui K, Motizuki M, Tsurugi K. The mechanism of action of ricin and related toxic lectins on eukaryotic ribosomes. The site and the characteristics of the modification in 28 S ribosomal RNA caused by the toxins. *J Biol Chem.* 1987 Apr 25;262(12):5908-12.
7. Sandvig K, Garred O, Prydz K, Kozlov JV, Hansen SH, van Deurs B. Retrograde transport of endocytosed Shiga toxin to the endoplasmic reticulum. *Nature.* 1992 Aug 6;358(6386):510-2.
8. Rapak A, Falnes PO, Olsnes S. Retrograde transport of mutant ricin to the endoplasmic reticulum with subsequent translocation to cytosol. *Proc Natl Acad Sci U S A.* 1997 Apr 15;94(8):3783-8.
9. van Deurs B, Pedersen LR, Sundan A, Olsnes S, Sandvig K. Receptor-mediated endocytosis of a ricin-colloidal gold conjugate in vero cells. Intracellular routing to vacuolar and tubulo-vesicular portions of the endosomal system. *Exp Cell Res.* 1985 Aug;159(2):287-304.
10. Sandvig K, Olsnes S, Petersen OW, van Deurs B. Acidification of the cytosol inhibits endocytosis from coated pits. *J Cell Biol.* 1987 Aug;105(2):679-89.
11. Larkin JM, Brown MS, Goldstein JL, Anderson RG. Depletion of intracellular potassium arrests coated pit formation and receptor-mediated endocytosis in fibroblasts. *Cell.* 1983 May;33(1):273-85.
12. Moya M, Dautry-Varsat A, Goud B, Louvard D, Boquet P. Inhibition of coated pit formation in Hep2 cells blocks the cytotoxicity of diphtheria toxin but not that of ricin toxin. *J Cell Biol.* 1985 Aug;101(2):548-59.
13. Llorente A, Rapak A, Schmid SL, van Deurs B, Sandvig K. Expression of mutant

- dynamain inhibits toxicity and transport of endocytosed ricin to the Golgi apparatus. *J Cell Biol.* 1998 Feb 9;140(3):553-63.
14. van Deurs B, Tonnessen TI, Petersen OW, Sandvig K, Olsnes S. Routing of internalized ricin and ricin conjugates to the Golgi complex. *J Cell Biol.* 1986 Jan;102(1):37-47.
 15. Lombardi D, Soldati T, Riederer MA, Goda Y, Zerial M, Pfeffer SR. Rab9 functions in transport between late endosomes and the trans Golgi network. *EMBO J.* 1993 Feb;12(2):677-82.
 16. Iversen TG, Skretting G, Llorente A, Nicoziani P, van Deurs B, Sandvig K. Endosome to Golgi transport of ricin is independent of clathrin and of the Rab9- and Rab11-GTPases. *Mol Biol Cell.* 2001 Jul;12(7):2099-107.
 17. Stechmann B, Bai SK, Gobbo E, Lopez R, Merer G, Pinchard S, et al. Inhibition of retrograde transport protects mice from lethal ricin challenge. *Cell.* 2010 Apr 16;141(2):231-42.
 18. Wales R, Roberts LM, Lord JM. Addition of an endoplasmic reticulum retrieval sequence to ricin A chain significantly increases its cytotoxicity to mammalian cells. *J Biol Chem.* 1993 Nov 15;268(32):23986-90.
 19. Wales R, Chaddock JA, Roberts LM, Lord JM. Addition of an ER retention signal to the ricin A chain increases the cytotoxicity of the holotoxin. *Exp Cell Res.* 1992 Nov;203(1):1-4.
 20. Peter F, Nguyen Van P, Soling HD. Different sorting of Lys-Asp-Glu-Leu proteins in rat liver. *J Biol Chem.* 1992 May 25;267(15):10631-7.
 21. Day PJ, Owens SR, Wesche J, Olsnes S, Roberts LM, Lord JM. An interaction between ricin and calreticulin that may have implications for toxin trafficking. *J Biol Chem.* 2001 Mar 9;276(10):7202-8.
 22. Roberts LM, Smith DC. Ricin: the endoplasmic reticulum connection. *Toxicon.* 2004 Oct;44(5):469-72.
 23. Sandvig K, van Deurs B. Entry of ricin and Shiga toxin into cells: molecular mechanisms and medical perspectives. *EMBO J.* 2000 Nov 15;19(22):5943-50.
 24. Olsnes S, Pihl A. Treatment of abrin and ricin with -mercaptoethanol opposite effects on their toxicity in mice and their ability to inhibit protein synthesis in a cell-free system. *FEBS Lett.* 1972 Nov 15;28(1):48-50.
 25. Day PJ, Pinheiro TJ, Roberts LM, Lord JM. Binding of ricin A-chain to negatively charged phospholipid vesicles leads to protein structural changes and destabilizes the lipid bilayer. *Biochemistry.* 2002 Feb 26;41(8):2836-43.

26. Deeks ED, Cook JP, Day PJ, Smith DC, Roberts LM, Lord JM. The low lysine content of ricin A chain reduces the risk of proteolytic degradation after translocation from the endoplasmic reticulum to the cytosol. *Biochemistry*. 2002 Mar 12;41(10):3405-13.
27. Argent RH, Parrott AM, Day PJ, Roberts LM, Stockley PG, Lord JM, et al. Ribosome-mediated folding of partially unfolded ricin A-chain. *J Biol Chem*. 2000 Mar 31;275(13):9263-9.
28. Walker D, Chaddock AM, Chaddock JA, Roberts LM, Lord JM, Robinson C. Ricin A chain fused to a chloroplast-targeting signal is unfolded on the chloroplast surface prior to import across the envelope membranes. *J Biol Chem*. 1996 Feb 23;271(8):4082-5.
29. Moazed D, Robertson JM, Noller HF. Interaction of elongation factors EF-G and EF-Tu with a conserved loop in 23S RNA. *Nature*. 1988 Jul 28;334(6180):362-4.
30. Holmberg L, Nygard O. Depurination of A4256 in 28 S rRNA by the ribosome-inactivating proteins from barley and ricin results in different ribosome conformations. *J Mol Biol*. 1996 May 31;259(1):81-94.
31. Sandvig K, van Deurs B. Endocytosis and intracellular transport of ricin: recent discoveries. *FEBS Lett*. 1999 Jun 4;452(1-2):67-70.
32. Li XP, Baricevic M, Saidasan H, Tumer NE. Ribosome depurination is not sufficient for ricin-mediated cell death in *Saccharomyces cerevisiae*. *Infect Immun*. 2007 Jan;75(1):417-28.
33. Jetzt AE, Cheng JS, Tumer NE, Cohick WS. Ricin A-chain requires c-Jun N-terminal kinase to induce apoptosis in nontransformed epithelial cells. *Int J Biochem Cell Biol*. 2009 Dec;41(12):2503-10.
34. Lin JY, Liu K, Chen CC, Tung TC. Effect of crystalline ricin on the biosynthesis of protein, RNA, and DNA in experimental tumor cells. *Cancer Res*. 1971 Jul;31(7):921-4.
35. Frankel AE, Burbage C, Fu T, Tagge E, Chandler J, Willingham M. Characterization of a ricin fusion toxin targeted to the interleukin-2 receptor. *Protein Eng*. 1996 Oct;9(10):913-9.
36. Vitetta ES, Fulton RJ, May RD, Till M, Uhr JW. Redesigning nature's poisons to create anti-tumor reagents. *Science*. 1987 Nov 20;238(4830):1098-104.
37. Bourrie BJ, Casellas P, Blythman HE, Jansen FK. Study of the plasma clearance of antibody--ricin-A-chain immunotoxins. Evidence for specific recognition sites on the A chain that mediate rapid clearance of the immunotoxin. *Eur J Biochem*. 1986 Feb

- 17;155(1):1-10.
38. Blakey DC, Watson GJ, Knowles PP, Thorpe PE. Effect of chemical deglycosylation of ricin A chain on the in vivo fate and cytotoxic activity of an immunotoxin composed of ricin A chain and anti-Thy 1.1 antibody. *Cancer Res.* 1987 Feb 15;47(4):947-52.
 39. Fulton RJ, Uhr JW, Vitetta ES. In vivo therapy of the BCL1 tumor: effect of immunotoxin valency and deglycosylation of the ricin A chain. *Cancer Res.* 1988 May 1;48(9):2626-31.
 40. Kuan CT, Pai LH, Pastan I. Immunotoxins containing Pseudomonas exotoxin that target LeY damage human endothelial cells in an antibody-specific mode: relevance to vascular leak syndrome. *Clin Cancer Res.* 1995 Dec;1(12):1589-94.
 41. Baluna R, Rizo J, Gordon BE, Ghetie V, Vitetta ES. Evidence for a structural motif in toxins and interleukin-2 that may be responsible for binding to endothelial cells and initiating vascular leak syndrome. *Proc Natl Acad Sci U S A.* 1999 Mar 30;96(7):3957-62.
 42. Misquittab CM, Mack, D. P. and Grover, A. K. . Sarco/endoplasmic reticulum Ca²⁺(SERCA)-pumps: link to heart beats and calcium waves. *cell calcium* 1999;25:277-90.
 43. Suzuki CK, Bonifacino JS, Lin AY, Davis MM, Klausner RD. Regulating the retention of T-cell receptor alpha chain variants within the endoplasmic reticulum: Ca²⁺-dependent association with BiP. *J Cell Biol.* 1991 Jul;114(2):189-205.
 44. Li LJ, Li X, Ferrario A, Rucker N, Liu ES, Wong S, et al. Establishment of a Chinese hamster ovary cell line that expresses grp78 antisense transcripts and suppresses A23187 induction of both GRP78 and GRP94. *J Cell Physiol.* 1992 Dec;153(3):575-82.
 45. Zhang JX, Braakman I, Matlack KE, Helenius A. Quality control in the secretory pathway: the role of calreticulin, calnexin and BiP in the retention of glycoproteins with C-terminal truncations. *Mol Biol Cell.* 1997 Oct;8(10):1943-54.
 46. Trombetta SE, Parodi AJ. Purification to apparent homogeneity and partial characterization of rat liver UDP-glucose:glycoprotein glucosyltransferase. *J Biol Chem.* 1992 May 5;267(13):9236-40.
 47. Kopito RR. ER quality control: the cytoplasmic connection. *Cell.* 1997 Feb 21;88(4):427-30.
 48. Plemper RK, Wolf DH. Retrograde protein translocation: ERADication of secretory proteins in health and disease. *Trends Biochem Sci.* 1999 Jul;24(7):266-70.

49. Pouyssegur J, Robert P. C. Shiua, and Ira Pastana. Induction of two transformation-sensitive membrane polypeptides in normal fibroblasts by a block in glycoprotein synthesis or glucose deprivation cell. 1977;11(4):941-7.
50. Lee AS. Mammalian stress response: induction of the glucose-regulated protein family. *Curr Opin Cell Biol.* 1992 Apr;4(2):267-73.
51. Kaufman RJ, Scheuner D, Schroder M, Shen X, Lee K, Liu CY, et al. The unfolded protein response in nutrient sensing and differentiation. *Nat Rev Mol Cell Biol.* 2002 Jun;3(6):411-21.
52. Vassilakos A, Michalak M, Lehrman MA, Williams DB. Oligosaccharide binding characteristics of the molecular chaperones calnexin and calreticulin. *Biochemistry.* 1998 Mar 10;37(10):3480-90.
53. Mori K. Tripartite management of unfolded proteins in the endoplasmic reticulum. *Cell.* 2000 May 26;101(5):451-4.
54. Patil C, Walter P. Intracellular signaling from the endoplasmic reticulum to the nucleus: the unfolded protein response in yeast and mammals. *Curr Opin Cell Biol.* 2001 Jun;13(3):349-55.
55. Brostrom CO, Brostrom MA. Regulation of translational initiation during cellular responses to stress. *Prog Nucleic Acid Res Mol Biol.* 1998;58:79-125.
56. Mori K. Signalling pathways in the unfolded protein response: development from yeast to mammals. *J Biochem.* 2009 Dec;146(6):743-50.
57. Yoshida H, Matsui T, Hosokawa N, Kaufman RJ, Nagata K, Mori K. A time-dependent phase shift in the mammalian unfolded protein response. *Dev Cell.* 2003 Feb;4(2):265-71.
58. Yamamoto K, Suzuki N, Wada T, Okada T, Yoshida H, Kaufman RJ, et al. Human HRD1 promoter carries a functional unfolded protein response element to which XBP1 but not ATF6 directly binds. *J Biochem.* 2008 Oct;144(4):477-86.
59. Kaneko M, Ishiguro M, Niinuma Y, Uesugi M, Nomura Y. Human HRD1 protects against ER stress-induced apoptosis through ER-associated degradation. *FEBS Lett.* 2002 Dec 4;532(1-2):147-52.
60. Lin JH, Li H, Yasumura D, Cohen HR, Zhang C, Panning B, et al. IRE1 signaling affects cell fate during the unfolded protein response. *Science.* 2007 Nov 9;318(5852):944-9.
61. Hetz C, Bernasconi P, Fisher J, Lee AH, Bassik MC, Antonsson B, et al. Proapoptotic BAX and BAK modulate the unfolded protein response by a direct interaction with IRE1alpha. *Science.* 2006 Apr 28;312(5773):572-6.

62. Rutkowski DT, Arnold SM, Miller CN, Wu J, Li J, Gunnison KM, et al. Adaptation to ER stress is mediated by differential stabilities of pro-survival and pro-apoptotic mRNAs and proteins. *PLoS Biol.* 2006 Nov;4(11):e374.
63. Nakagawa T, Zhu H, Morishima N, Li E, Xu J, Yankner BA, et al. Caspase-12 mediates endoplasmic-reticulum-specific apoptosis and cytotoxicity by amyloid-beta. *Nature.* 2000 Jan 6;403(6765):98-103.
64. Urano F, Wang X, Bertolotti A, Zhang Y, Chung P, Harding HP, et al. Coupling of stress in the ER to activation of JNK protein kinases by transmembrane protein kinase IRE1. *Science.* 2000 Jan 28;287(5453):664-6.
65. Lei K, Davis RJ. JNK phosphorylation of Bim-related members of the Bcl2 family induces Bax-dependent apoptosis. *Proc Natl Acad Sci U S A.* 2003 Mar 4;100(5):2432-7.
66. Putcha GV, Le S, Frank S, Besirli CG, Clark K, Chu B, et al. JNK-mediated BIM phosphorylation potentiates BAX-dependent apoptosis. *Neuron.* 2003 Jun 19;38(6):899-914.
67. Reimertz C, Kogel D, Rami A, Chittenden T, Prehn JH. Gene expression during ER stress-induced apoptosis in neurons: induction of the BH3-only protein Bbc3/PUMA and activation of the mitochondrial apoptosis pathway. *J Cell Biol.* 2003 Aug 18;162(4):587-97.
68. Li J, Lee B, Lee AS. Endoplasmic reticulum stress-induced apoptosis: multiple pathways and activation of p53-up-regulated modulator of apoptosis (PUMA) and NOXA by p53. *J Biol Chem.* 2006 Mar 17;281(11):7260-70.
69. Puthalakath H, O'Reilly LA, Gunn P, Lee L, Kelly PN, Huntington ND, et al. ER stress triggers apoptosis by activating BH3-only protein Bim. *Cell.* 2007 Jun 29;129(7):1337-49.
70. McCullough KD, Martindale JL, Klotz LO, Aw TY, Holbrook NJ. Gadd153 sensitizes cells to endoplasmic reticulum stress by down-regulating Bcl2 and perturbing the cellular redox state. *Mol Cell Biol.* 2001 Feb;21(4):1249-59.
71. Zinszner H, Kuroda M, Wang X, Batchvarova N, Lightfoot RT, Remotti H, et al. CHOP is implicated in programmed cell death in response to impaired function of the endoplasmic reticulum. *Genes Dev.* 1998 Apr 1;12(7):982-95.
72. Orrenius S, Zhivotovsky B, Nicotera P. Regulation of cell death: the calcium-apoptosis link. *Nat Rev Mol Cell Biol.* 2003 Jul;4(7):552-65.
73. Filippin L, Magalhães, Paulo J. , Giuletta Di Benedetto, Matilde Colella and Tullio Pozzan. Stable Interactions between Mitochondria and Endoplasmic Reticulum

- Allow Rapid Accumulation of Calcium in a Subpopulation of Mitochondria. *Journal of Biological Chemistry*. 2003;278:39224-34.
74. Harding HP, Zeng H, Zhang Y, Jungries R, Chung P, Plesken H, et al. Diabetes mellitus and exocrine pancreatic dysfunction in *perk*^{-/-} mice reveals a role for translational control in secretory cell survival. *Mol Cell*. 2001 Jun;7(6):1153-63.
 75. Zhang P, McGrath B, Li S, Frank A, Zambito F, Reinert J, et al. The PERK eukaryotic initiation factor 2 alpha kinase is required for the development of the skeletal system, postnatal growth, and the function and viability of the pancreas. *Mol Cell Biol*. 2002 Jun;22(11):3864-74.
 76. Delepine M, Nicolino M, Barrett T, Golamaully M, Lathrop GM, Julier C. EIF2AK3, encoding translation initiation factor 2-alpha kinase 3, is mutated in patients with Wolcott-Rallison syndrome. *Nat Genet*. 2000 Aug;25(4):406-9.
 77. Ozcan U, Cao Q, Yilmaz E, Lee AH, Iwakoshi NN, Ozdelen E, et al. Endoplasmic reticulum stress links obesity, insulin action, and type 2 diabetes. *Science*. 2004 Oct 15;306(5695):457-61.
 78. Kim I, Xu W, Reed JC. Cell death and endoplasmic reticulum stress: disease relevance and therapeutic opportunities. *Nat Rev Drug Discov*. 2008 Dec;7(12):1013-30.
 79. Fujimoto T, Onda M, Nagai H, Nagahata T, Ogawa K, Emi M. Upregulation and overexpression of human X-box binding protein 1 (hXBP-1) gene in primary breast cancers. *Breast Cancer*. 2003;10(4):301-6.
 80. Shuda M, Kondoh N, Imazeki N, Tanaka K, Okada T, Mori K, et al. Activation of the ATF6, XBP1 and grp78 genes in human hepatocellular carcinoma: a possible involvement of the ER stress pathway in hepatocarcinogenesis. *J Hepatol*. 2003 May;38(5):605-14.
 81. Jamora C, Dennert G, Lee AS. Inhibition of tumor progression by suppression of stress protein GRP78/BiP induction in fibrosarcoma B/C10ME. *Proc Natl Acad Sci U S A*. 1996 Jul 23;93(15):7690-4.
 82. Romero-Ramirez LHC, Daniel Nelson, Ester Hammond, Ann-Hwee Lee, Hiderou Yoshida,, Kazutoshi Mori LHG, Nicholas C. Denko, Amato J. Giaccia, Quynh-Thu Le, Albert C. Koong1. XBP1 Is Essential for Survival under Hypoxic Conditions and Is Required for Tumor Growth. *cancer research*. 2004;64:5943-7.
 83. Bi M, Naczki C, Koritzinsky M, Fels D, Blais J, Hu N, et al. ER stress-regulated translation increases tolerance to extreme hypoxia and promotes tumor growth. *EMBO J*. 2005 Oct 5;24(19):3470-81.

84. Cox JS, Shamu CE, Walter P. Transcriptional induction of genes encoding endoplasmic reticulum resident proteins requires a transmembrane protein kinase. *Cell*. 1993 Jun 18;73(6):1197-206.
85. Mori K, Ma, W., Gething, M. J., Sambrook, J. A transmembrane protein with a cdc2+/CDC28-related kinase activity is required for signaling from the ER to the nucleus. *Cell*. 1993 Aug 27;74(4):743-56.
86. Shamu CE, Walter P. Oligomerization and phosphorylation of the Ire1p kinase during intracellular signaling from the endoplasmic reticulum to the nucleus. *EMBO J*. 1996 Jun 17;15(12):3028-39.
87. Welihinda AA, Kaufman RJ. The unfolded protein response pathway in *Saccharomyces cerevisiae*. Oligomerization and trans-phosphorylation of Ire1p (Ern1p) are required for kinase activation. *J Biol Chem*. 1996 Jul 26;271(30):18181-7.
88. Dong B, Xu, L., Zhou, A., Hassel, B.A., Lee, X., Torrence, P.F., and Silverman, R.H. Intrinsic molecular activities of the interferon-induced 2–5A dependent RNase. *J Biol Chem*. 1994;269:14153–8.
89. Sidrauski C, Walter P. The transmembrane kinase Ire1p is a site-specific endonuclease that initiates mRNA splicing in the unfolded protein response. *Cell*. 1997 Sep 19;90(6):1031-9.
90. Cox JS, Walter P. A novel mechanism for regulating activity of a transcription factor that controls the unfolded protein response. *Cell*. 1996 Nov 1;87(3):391-404.
91. Nikawa J, Akiyoshi M, Hirata S, Fukuda T. *Saccharomyces cerevisiae* IRE2/HAC1 is involved in IRE1-mediated KAR2 expression. *Nucleic Acids Res*. 1996 Nov 1;24(21):4222-6.
92. Kawahara T, Yanagi H, Yura T, Mori K. Unconventional splicing of HAC1/ERN4 mRNA required for the unfolded protein response. Sequence-specific and non-sequential cleavage of the splice sites. *J Biol Chem*. 1998 Jan 16;273(3):1802-7.
93. Sidrauski C, Cox JS, Walter P. tRNA ligase is required for regulated mRNA splicing in the unfolded protein response. *Cell*. 1996 Nov 1;87(3):405-13.
94. Mori K, Ogawa N, Kawahara T, Yanagi H, Yura T. Palindrome with spacer of one nucleotide is characteristic of the cis-acting unfolded protein response element in *Saccharomyces cerevisiae*. *J Biol Chem*. 1998 Apr 17;273(16):9912-20.
95. Chapman RE, Walter P. Translational attenuation mediated by an mRNA intron. *Curr Biol*. 1997 Nov 1;7(11):850-9.
96. Tirasophon W, Welihinda AA, Kaufman RJ. A stress response pathway from the

- endoplasmic reticulum to the nucleus requires a novel bifunctional protein kinase/endoribonuclease (Ire1p) in mammalian cells. *Genes Dev.* 1998 Jun 15;12(12):1812-24.
97. Wang XZ, Harding HP, Zhang Y, Jolicoeur EM, Kuroda M, Ron D. Cloning of mammalian Ire1 reveals diversity in the ER stress responses. *EMBO J.* 1998 Oct 1;17(19):5708-17.
 98. Wang XZ, Kuroda M, Sok J, Batchvarova N, Kimmel R, Chung P, et al. Identification of novel stress-induced genes downstream of chop. *EMBO J.* 1998 Jul 1;17(13):3619-30.
 99. Yoshida H, Matsui T, Yamamoto A, Okada T, Mori K. XBP1 mRNA is induced by ATF6 and spliced by IRE1 in response to ER stress to produce a highly active transcription factor. *Cell.* 2001 Dec 28;107(7):881-91.
 100. Lee K, Tirasophon W, Shen X, Michalak M, Prywes R, Okada T, et al. IRE1-mediated unconventional mRNA splicing and S2P-mediated ATF6 cleavage merge to regulate XBP1 in signaling the unfolded protein response. *Genes Dev.* 2002 Feb 15;16(4):452-66.
 101. Calton M, Zeng H, Urano F, Till JH, Hubbard SR, Harding HP, et al. IRE1 couples endoplasmic reticulum load to secretory capacity by processing the XBP-1 mRNA. *Nature.* 2002 Jan 3;415(6867):92-6.
 102. Credle JJ, Finer-Moore JS, Papa FR, Stroud RM, Walter P. On the mechanism of sensing unfolded protein in the endoplasmic reticulum. *Proc Natl Acad Sci U S A.* 2005 Dec 27;102(52):18773-84.
 103. Zhou J, Liu CY, Back SH, Clark RL, Peisach D, Xu Z, et al. The crystal structure of human IRE1 luminal domain reveals a conserved dimerization interface required for activation of the unfolded protein response. *Proc Natl Acad Sci U S A.* 2006 Sep 26;103(39):14343-8.
 104. Korennykh AV, Egea PF, Korostelev AA, Finer-Moore J, Zhang C, Shokat KM, et al. The unfolded protein response signals through high-order assembly of Ire1. *Nature.* 2009 Feb 5;457(7230):687-93.
 105. Oikawa D, Kimata Y, Kohno K, Iwawaki T. Activation of mammalian IRE1alpha upon ER stress depends on dissociation of BiP rather than on direct interaction with unfolded proteins. *Exp Cell Res.* 2009 Sep 10;315(15):2496-504.
 106. Bertolotti A ZY, Hendershot LM, Harding HP, Ron D. Dynamic interaction of BiP and ER stress transducers in the unfolded-protein response. *Nat Cell Biol.* 2000;2:326-32.

107. Morris JA DA, Edward CA, Hendershot LM and Kaufman RJ. Immunoglobulin Binding Protein (BiP) Function Is Required to Protect Cells from Endoplasmic Reticulum Stress but Is Not Required for the Secretion of Selective Proteins. *journal of biological chemistry*. 1997;272:4327-34.
108. Lee KP, Dey M, Neculai D, Cao C, Dever TE, Sicheri F. Structure of the dual enzyme Ire1 reveals the basis for catalysis and regulation in nonconventional RNA splicing. *Cell*. 2008 Jan 11;132(1):89-100.
109. Gonzalez TN, Sidrauski C, Dorfler S, Walter P. Mechanism of non-spliceosomal mRNA splicing in the unfolded protein response pathway. *EMBO J*. 1999 Jun 1;18(11):3119-32.
110. Ruegsegger U, Leber JH, Walter P. Block of HAC1 mRNA translation by long-range base pairing is released by cytoplasmic splicing upon induction of the unfolded protein response. *Cell*. 2001 Oct 5;107(1):103-14.
111. Tirasophon W, Lee K, Callaghan B, Welihinda A, Kaufman RJ. The endoribonuclease activity of mammalian IRE1 autoregulates its mRNA and is required for the unfolded protein response. *Genes Dev*. 2000 Nov 1;14(21):2725-36.
112. Yoshida H, Okada T, Haze K, Yanagi H, Yura T, Negishi M, et al. ATF6 activated by proteolysis binds in the presence of NF-Y (CBF) directly to the cis-acting element responsible for the mammalian unfolded protein response. *Mol Cell Biol*. 2000 Sep;20(18):6755-67.
113. Lee AH, Iwakoshi NN, Glimcher LH. XBP-1 regulates a subset of endoplasmic reticulum resident chaperone genes in the unfolded protein response. *Mol Cell Biol*. 2003 Nov;23(21):7448-59.
114. Yamamoto K, Yoshida H, Kokame K, Kaufman RJ, Mori K. Differential contributions of ATF6 and XBP1 to the activation of endoplasmic reticulum stress-responsive cis-acting elements ERSE, UPR and ERSE-II. *J Biochem*. 2004 Sep;136(3):343-50.
115. Wang Y, Shen J, Arenzana N, Tirasophon W, Kaufman RJ, Prywes R. Activation of ATF6 and an ATF6 DNA binding site by the endoplasmic reticulum stress response. *J Biol Chem*. 2000 Sep 1;275(35):27013-20.
116. Yoshida H, Oku M, Suzuki M, Mori K. pXBP1(U) encoded in XBP1 pre-mRNA negatively regulates unfolded protein response activator pXBP1(S) in mammalian ER stress response. *J Cell Biol*. 2006 Feb 13;172(4):565-75.
117. Nishitoh H, Matsuzawa A, Tobiume K, Saegusa K, Takeda K, Inoue K, et al. ASK1 is essential for endoplasmic reticulum stress-induced neuronal cell death triggered by

- expanded polyglutamine repeats. *Genes Dev.* 2002 Jun 1;16(11):1345-55.
118. Luo D, He Y, Zhang H, Yu L, Chen H, Xu Z, et al. AIP1 is critical in transducing IRE1-mediated endoplasmic reticulum stress response. *J Biol Chem.* 2008 May 2;283(18):11905-12.
119. Haze K, Yoshida H, Yanagi H, Yura T, Mori K. Mammalian transcription factor ATF6 is synthesized as a transmembrane protein and activated by proteolysis in response to endoplasmic reticulum stress. *Mol Biol Cell.* 1999 Nov;10(11):3787-99.
120. Ye J, Rawson RB, Komuro R, Chen X, Dave UP, Prywes R, et al. ER stress induces cleavage of membrane-bound ATF6 by the same proteases that process SREBPs. *Mol Cell.* 2000 Dec;6(6):1355-64.
121. Thuerauf DJ, Morrison LE, Hoover H, Glembotski CC. Coordination of ATF6-mediated transcription and ATF6 degradation by a domain that is shared with the viral transcription factor, VP16. *J Biol Chem.* 2002 Jun 7;277(23):20734-9.
122. Bause E. Structural requirements of N-glycosylation of proteins. Studies with proline peptides as conformational probes. *Biochem J.* 1983 Feb 1;209(2):331-6.
123. Hong M, Luo S, Baumeister P, Huang JM, Gogia RK, Li M, et al. Underglycosylation of ATF6 as a novel sensing mechanism for activation of the unfolded protein response. *J Biol Chem.* 2004 Mar 19;279(12):11354-63.
124. Chen X, Shen J, Prywes R. The luminal domain of ATF6 senses endoplasmic reticulum (ER) stress and causes translocation of ATF6 from the ER to the Golgi. *J Biol Chem.* 2002 Apr 12;277(15):13045-52.
125. Shen J, Chen X, Hendershot L, Prywes R. ER stress regulation of ATF6 localization by dissociation of BiP/GRP78 binding and unmasking of Golgi localization signals. *Dev Cell.* 2002 Jul;3(1):99-111.
126. Nakanaka S, Yoshida H, Kano F, Murata M, Mori K. Activation of mammalian unfolded protein response is compatible with the quality control system operating in the endoplasmic reticulum. *Mol Biol Cell.* 2004 Jun;15(6):2537-48.
127. Wang X, Sato R, Brown MS, Hua X, Goldstein JL. SREBP-1, a membrane-bound transcription factor released by sterol-regulated proteolysis. *Cell.* 1994 Apr 8;77(1):53-62.
128. Sakai J, Duncan EA, Rawson RB, Hua X, Brown MS, Goldstein JL. Sterol-regulated release of SREBP-2 from cell membranes requires two sequential cleavages, one within a transmembrane segment. *Cell.* 1996 Jun 28;85(7):1037-46.
129. Haze K, Okada T, Yoshida H, Yanagi H, Yura T, Negishi M, et al. Identification of the G13 (cAMP-response-element-binding protein-related protein) gene product related

- to activating transcription factor 6 as a transcriptional activator of the mammalian unfolded protein response. *Biochem J.* 2001 Apr 1;355(Pt 1):19-28.
130. Yamamoto K, Sato T, Matsui T, Sato M, Okada T, Yoshida H, et al. Transcriptional induction of mammalian ER quality control proteins is mediated by single or combined action of ATF6alpha and XBP1. *Dev Cell.* 2007 Sep;13(3):365-76.
 131. Thuerauf DJ, Morrison L, Glembotski CC. Opposing roles for ATF6alpha and ATF6beta in endoplasmic reticulum stress response gene induction. *J Biol Chem.* 2004 May 14;279(20):21078-84.
 132. Harding HP, Zhang Y, Ron D. Protein translation and folding are coupled by an endoplasmic-reticulum-resident kinase. *Nature.* 1999 Jan 21;397(6716):271-4.
 133. Liu CY, Schroder M, Kaufman RJ. Ligand-independent dimerization activates the stress response kinases IRE1 and PERK in the lumen of the endoplasmic reticulum. *J Biol Chem.* 2000 Aug 11;275(32):24881-5.
 134. Su Q, Wang S, Gao HQ, Kazemi S, Harding HP, Ron D, et al. Modulation of the eukaryotic initiation factor 2 alpha-subunit kinase PERK by tyrosine phosphorylation. *J Biol Chem.* 2008 Jan 4;283(1):469-75.
 135. Shi Y, Vattem KM, Sood R, An J, Liang J, Stramm L, et al. Identification and characterization of pancreatic eukaryotic initiation factor 2 alpha-subunit kinase, PEK, involved in translational control. *Mol Cell Biol.* 1998 Dec;18(12):7499-509.
 136. Clemens MJ. Regulation of eukaryotic protein synthesis by protein kinases that phosphorylate initiation factor eIF-2. *Mol Biol Rep.* 1994 May;19(3):201-10.
 137. Sherr CJ. G1 phase progression: cycling on cue. *Cell.* 1994 Nov 18;79(4):551-5.
 138. Brewer JW, Hendershot LM, Sherr CJ, Diehl JA. Mammalian unfolded protein response inhibits cyclin D1 translation and cell-cycle progression. *Proc Natl Acad Sci U S A.* 1999 Jul 20;96(15):8505-10.
 139. Harding HP, Novoa I, Zhang Y, Zeng H, Wek R, Schapira M, et al. Regulated translation initiation controls stress-induced gene expression in mammalian cells. *Mol Cell.* 2000 Nov;6(5):1099-108.
 140. Vattem KM, Wek RC. Reinitiation involving upstream ORFs regulates ATF4 mRNA translation in mammalian cells. *Proc Natl Acad Sci U S A.* 2004 Aug 3;101(31):11269-74.
 141. Lu PD, Harding HP, Ron D. Translation reinitiation at alternative open reading frames regulates gene expression in an integrated stress response. *J Cell Biol.* 2004 Oct 11;167(1):27-33.
 142. Ma Y, Brewer JW, Diehl JA, Hendershot LM. Two distinct stress signaling pathways

- converge upon the CHOP promoter during the mammalian unfolded protein response. *J Mol Biol.* 2002 May 17;318(5):1351-65.
143. Jiang HY, Wek SA, McGrath BC, Lu D, Hai T, Harding HP, et al. Activating transcription factor 3 is integral to the eukaryotic initiation factor 2 kinase stress response. *Mol Cell Biol.* 2004 Feb;24(3):1365-77.
 144. Cullinan SB, Zhang D, Hannink M, Arvisais E, Kaufman RJ, Diehl JA. Nrf2 is a direct PERK substrate and effector of PERK-dependent cell survival. *Mol Cell Biol.* 2003 Oct;23(20):7198-209.
 145. Itoh K, Wakabayashi N, Katoh Y, Ishii T, Igarashi K, Engel JD, et al. Keap1 represses nuclear activation of antioxidant responsive elements by Nrf2 through binding to the amino-terminal Neh2 domain. *Genes Dev.* 1999 Jan 1;13(1):76-86.
 146. He CH, Gong P, Hu B, Stewart D, Choi ME, Choi AM, et al. Identification of activating transcription factor 4 (ATF4) as an Nrf2-interacting protein. Implication for heme oxygenase-1 gene regulation. *J Biol Chem.* 2001 Jun 15;276(24):20858-65.
 147. Itoh K, Chiba T, Takahashi S, Ishii T, Igarashi K, Katoh Y, et al. An Nrf2/small Maf heterodimer mediates the induction of phase II detoxifying enzyme genes through antioxidant response elements. *Biochem Biophys Res Commun.* 1997 Jul 18;236(2):313-22.
 148. Nguyen T, Huang HC, Pickett CB. Transcriptional regulation of the antioxidant response element. Activation by Nrf2 and repression by MafK. *J Biol Chem.* 2000 May 19;275(20):15466-73.
 149. Venugopal R, Jaiswal AK. Nrf2 and Nrf1 in association with Jun proteins regulate antioxidant response element-mediated expression and coordinated induction of genes encoding detoxifying enzymes. *Oncogene.* 1998 Dec 17;17(24):3145-56.
 150. Yan W, Frank CL, Korth MJ, Sopher BL, Novoa I, Ron D, et al. Control of PERK eIF2alpha kinase activity by the endoplasmic reticulum stress-induced molecular chaperone P58IPK. *Proc Natl Acad Sci U S A.* 2002 Dec 10;99(25):15920-5.
 151. Ma K, Vattam KM, Wek RC. Dimerization and release of molecular chaperone inhibition facilitate activation of eukaryotic initiation factor-2 kinase in response to endoplasmic reticulum stress. *J Biol Chem.* 2002 May 24;277(21):18728-35.
 152. Novoa I, Zeng H, Harding HP, Ron D. Feedback inhibition of the unfolded protein response by GADD34-mediated dephosphorylation of eIF2alpha. *J Cell Biol.* 2001 May 28;153(5):1011-22.
 153. Brush MH, Weiser DC, Shenolikar S. Growth arrest and DNA damage-inducible protein GADD34 targets protein phosphatase 1 alpha to the endoplasmic reticulum

- and promotes dephosphorylation of the alpha subunit of eukaryotic translation initiation factor 2. *Mol Cell Biol.* 2003 Feb;23(4):1292-303.
154. Parikh BA, Tortora A, Li XP, Tumer NE. Ricin inhibits activation of the unfolded protein response by preventing splicing of the HAC1 mRNA. *J Biol Chem.* 2008 Mar 7;283(10):6145-53.
 155. Huynh HT, Robitaille G, Turner JD. Establishment of bovine mammary epithelial cells (MAC-T): an in vitro model for bovine lactation. *Exp Cell Res.* 1991 Dec;197(2):191-9.
 156. Grill CJ, Sivaprasad U, Cohick WS. Constitutive expression of IGF-binding protein-3 by mammary epithelial cells alters signaling through Akt and p70S6 kinase. *J Mol Endocrinol.* 2002 Aug;29(1):153-62.
 157. Lee SY, Lee MS, Cherla RP, Tesh VL. Shiga toxin 1 induces apoptosis through the endoplasmic reticulum stress response in human monocytic cells. *Cell Microbiol.* 2008 Mar;10(3):770-80.
 158. Harama D, Koyama K, Mukai M, Shimokawa N, Miyata M, Nakamura Y, et al. A subcytotoxic dose of subtilase cytotoxin prevents lipopolysaccharide-induced inflammatory responses, depending on its capacity to induce the unfolded protein response. *J Immunol.* 2009 Jul 15;183(2):1368-74.
 159. Hu CC, Dougan SK, Winter SV, Paton AW, Paton JC, Ploegh HL. Subtilase cytotoxin cleaves newly synthesized BiP and blocks antibody secretion in B lymphocytes. *J Exp Med.* 2009 Oct 26;206(11):2429-40.
 160. Barbieri L, Valbonesi P, Bonora E, Gorini P, Bolognesi A, Stirpe F. Polynucleotide:adenosine glycosidase activity of ribosome-inactivating proteins: effect on DNA, RNA and poly(A). *Nucleic Acids Res.* 1997 Feb 1;25(3):518-22.
 161. Gill DL, Waldron RT, Rys-Sikora KE, Ufret-Vincenty CA, Graber MN, Favre CJ, et al. Calcium pools, calcium entry, and cell growth. *Biosci Rep.* 1996 Apr;16(2):139-57.
 162. Wesche J, Rapak A, Olsnes S. Dependence of ricin toxicity on translocation of the toxin A-chain from the endoplasmic reticulum to the cytosol. *J Biol Chem.* 1999 Nov 26;274(48):34443-9.
 163. Rose MD, Misra LM, Vogel JP. KAR2, a karyogamy gene, is the yeast homolog of the mammalian BiP/GRP78 gene. *Cell.* 1989 Jun 30;57(7):1211-21.
 164. Reddy RK, Mao C, Baumeister P, Austin RC, Kaufman RJ, Lee AS. Endoplasmic reticulum chaperone protein GRP78 protects cells from apoptosis induced by topoisomerase inhibitors: role of ATP binding site in suppression of caspase-7

- activation. *J Biol Chem.* 2003 Jun 6;278(23):20915-24.
165. Lee AS. The ER chaperone and signaling regulator GRP78/BiP as a monitor of endoplasmic reticulum stress. *Methods.* 2005 Apr;35(4):373-81.
166. Lee AS, Hendershot LM. ER stress and cancer. *Cancer Biol Ther.* 2006 Jul;5(7):721-2.
167. Pyrko P, Schonthal AH, Hofman FM, Chen TC, Lee AS. The unfolded protein response regulator GRP78/BiP as a novel target for increasing chemosensitivity in malignant gliomas. *Cancer Res.* 2007 Oct 15;67(20):9809-16.
168. Schroder M, Kaufman RJ. ER stress and the unfolded protein response. *Mutat Res.* 2005 Jan 6;569(1-2):29-63.